

INVARIANTS OF LEGENDRIAN KNOTS IN CIRCLE BUNDLES

JOSHUA M. SABLOFF

ABSTRACT. Let M be a circle bundle over a Riemann surface that supports a contact structure transverse to the fibers. This paper presents a combinatorial definition of a differential graded algebra (DGA) that is an invariant of Legendrian knots in M . The invariant generalizes Chekanov's combinatorial DGA invariant of Legendrian knots in the standard contact 3-space using ideas from Eliashberg, Givental, and Hofer's contact homology. The main difficulty lies in dealing with what are ostensibly 1-parameter families of generators for the DGA; these are solved using "Morse-Bott" techniques. As an application, the invariant is used to distinguish two Legendrian knots that are smoothly isotopic, realize a non-trivial homology class, but are not Legendrian isotopic.

CONTENTS

1. Introduction	2
1.1. Legendrian Knots	2
1.2. Combinatorial Contact Homology	2
2. Geometry of Contact Circle Bundles	4
2.1. Basic Notions of Contact Geometry	4
2.2. Diagrams of Legendrian Knots	5
3. A Combinatorial Definition of the Invariant	9
3.1. The Underlying Algebra \mathcal{A}	9
3.2. The Differential on \mathcal{A}	12
3.3. A Simple Example	16
3.4. Algebraic Notions	18
4. Applications	20
4.1. An Example with Nontrivial Degree in the Fiber	20
4.2. An Example with Nontrivial Homology in the Base	21
5. Proof that \mathcal{A} is a DGA	22
5.1. Outline of the Proof	22
5.2. An Equivalent Definition of ∂	23
5.3. Gluing Broken Disks	27
5.4. Degeneration of Obtuse Disks	28
6. Proof of Invariance	34
6.1. Choices at c and d Points	34
6.2. Legendrian Isotopy	38
Acknowledgments	48
References	48

1. INTRODUCTION

1.1. Legendrian Knots. A Legendrian knot is a smooth embedding of the circle into a contact manifold that is everywhere tangent to the contact planes.¹ One fundamental problem in Legendrian knot theory is to determine when two Legendrian knots are not (or are) isotopic through Legendrian knots, even if they are isotopic as smooth knots. In other words, the problem is to find effective invariants of Legendrian isotopy. For null-homologous knots, the first step is to define the the Thurston-Bennequin and rotation numbers (the so-called “classical invariants”). Eliashberg and Fraser proved that these two invariants classify unknots in tight contact 3-manifolds [10], and Etnyre and Honda proved that the classical invariants also classify the Legendrian figure eight knots and torus knots [15].

The classical invariants are not the whole story, however. Chekanov [5] built an invariant of Legendrian isotopy that distinguishes two Legendrian 5_2 knots that have the same classical invariants. Chekanov’s invariant (commonly referred to as the Chekanov-Eliashberg algebra) is a non-commutative differential graded algebra (DGA) over \mathbb{Z}_2 , freely generated by the double points of the xy diagram of a Legendrian knot. The differential comes from counting immersed polygons with corners at the double points and whose edges lie in the diagram. The “stable tame isomorphism” type — and consequently the homology — of the DGA is invariant under Legendrian isotopy. It is difficult to extract information from this invariant, but Chekanov defined a “linearized” theory of the DGA that, when it exists, has proven to be useful in distinguishing Legendrian knots that have the same classical invariants; also see Fuchs et al. [13, 18]. In [22], Ng generated more powerful methods for mining the DGA for information and used them to distinguish Legendrian knots that the linearized DGA cannot.

At the same time that Chekanov was developing his invariant, Eliashberg, Givental, and Hofer [11] constructed a geometric invariant for Legendrian knots.² Their **relative contact homology** is a non-commutative DGA generated by the Reeb chords of the knot (in a sufficiently generic setup in which the chords are isolated). For a contact manifold (M, α) , let $(M \times \mathbb{R}, d(e^t \alpha))$ be its symplectization; if L is a Legendrian knot in M , then $L \times \mathbb{R}$ is a Lagrangian submanifold of the symplectization. The differential for the DGA is defined by counting rigid J -holomorphic disks in $M \times \mathbb{R}$ whose boundaries lie in $L \times \mathbb{R}$. In [16], it was proven that Chekanov’s invariant is a combinatorial translation of Eliashberg, Givental, and Hofer’s contact homology for the standard contact structure on \mathbb{R}^3 .

Whereas the classification results of Eliashberg-Fraser and Etnyre-Honda hold in any tight contact manifold, thus far, non-classical invariants have been rendered computable only for the standard structure on \mathbb{R}^3 and for the space of contact elements to the plane. The results in this paper use the ideas of relative contact homology to extend the range of tight manifolds for which there is a combinatorially computable non-classical invariant. In particular, the goal of this paper is to define a combinatorial theory for Legendrian knots in circle bundles that have contact structures transverse to their fibers.

1.2. Combinatorial Contact Homology. The key feature used in defining a combinatorial translation of relative contact homology is that the projection along the Reeb flow is a fibration over a complex base. For example, in the \mathbb{R}^3 case, the Reeb field points along the positive z direction. Thus, the projection along the Reeb flow is equivalent to projection to the xy plane. Consequently, the Reeb chords of a knot correspond to the double points of its xy diagram, which shows that

¹See Section 2.1 for more of the basic notions of contact geometry.

²Givental’s contributions to the theory came after the name “Chekanov-Eliashberg algebra” came into common usage, but the reasons that Hofer’s name was omitted are lost in the sands of time.

the generators of the Chekanov-Eliashberg algebra are the same as those of the relative contact homology algebra. The fact that the projection from the almost complex manifold $(M \times \mathbb{R}, J)$ to the base of the fibration is holomorphic leads to a correspondence between spaces of immersed polygons used to define the combinatorial differential and the moduli spaces of rigid holomorphic disks in the geometric theory. See Section 7 of [16] for more details.

Circle bundles with a contact structure transverse to their fibers constitutes another class of contact manifolds for which the Reeb flow induces a fibration. For these **contact circle bundles**, a contact form may be chosen so that the Reeb field points along the fibers.³ Thus, the projection along the Reeb flow is the same as the bundle projection to the base. Eliashberg, Givental, and Hofer's theory says that the DGA of a Legendrian knot L should be generated by the Reeb chords. There are two types of Reeb chords for a Legendrian knot in a contact circle bundle. The first type come from double points of the projection of L to the base. Over a double point, there are chords that start on one strand of L , possibly wrap around the fiber a few times, and finish on the other strand. These are isolated, and to each double point there corresponds two sets of chords, depending on the starting strand. Each set is indexed by the winding number of the chord around the fiber. The second type live over every point of L : they start and end at the same point, traversing the fiber at least once. For each winding number around the fiber, there is a 1-parameter family of these chords, parameterized by L . This would seem to indicate that the DGA would have to be uncountably generated.

In order to deal with this complication, "Morse-Bott" methods must be applied to relative contact homology. In particular, each 1-parameter family is replaced by the critical points of a Morse function on that family, and the differential is adjusted to reflect this perturbation. These techniques lead to the following theorem:

Theorem 1.1. *Let (E, α) be a contact circle bundle. Let L be a Legendrian knot in (E, α) . Then there is a combinatorially-defined filtered DGA whose "stable tame isomorphism" type is invariant under Legendrian isotopy of L .*

The combinatorial definition of the invariant occupies Section 3, and Theorem 3.11 states that the invariant is a genuine DGA. The definitions necessary to understand the invariance properties of the DGA are set out in Section 3.4, culminating in Theorem 3.15.

As an application, the invariant of Theorem 1.1 may be used to prove:

Proposition 1.2. *There exist examples of Legendrian knots in circle bundles that are smoothly isotopic but not Legendrian isotopic that, additionally, satisfy one of the following two topological properties:*

1. *The knot has nontrivial degree in the fiber.*
2. *The projection of the knot to the base F represents a nontrivial homology class.*

The remainder of the paper is divided into five sections. Section 2 surveys the basic notions of contact geometry and, in particular, the geometry of contact structures on circle bundles. The section ends with a combinatorial description of the projection of a Legendrian knot to the base, paying particular attention to the case of knots in lens spaces.

In Section 3, the definition of the DGA appears in three parts: first, the underlying algebra is defined in Section 3.1. Second, the differential is described in Section 3.2, with a simple example to illustrate how to compute it in Section 3.3. Finally, the algebraic notions necessary for the statement of invariance are detailed in Section 3.4. As mentioned above, the two most important theorems are Theorems 3.11 and 3.15, which combine to make Theorem 1.1 precise. The proofs of

³See Section 2.1 for a more detailed construction of these contact structures.

these theorems are delayed until Sections 5 and 6, respectively. Section 4 contains the computations necessary to prove Proposition 1.2.

2. GEOMETRY OF CONTACT CIRCLE BUNDLES

2.1. Basic Notions of Contact Geometry. Let M be a closed, oriented 3-manifold. A **contact structure** ξ on M is a completely non-integrable tangent 2-plane field. If ξ is the kernel of a 1-form α , then the non-integrability condition is equivalent to $\alpha \wedge d\alpha$ being nowhere vanishing. Such a contact structure is called **co-oriented** and α is called a **contact form**. A co-oriented contact structure is called **positive** if $\alpha \wedge d\alpha$ gives the correct orientation on M . A contact form picks out a special vector field transverse to ξ called the **Reeb field** X_α . This vector field is defined by the equations

$$\begin{aligned} d\alpha(X_\alpha, \cdot) &= 0, \\ \alpha(X_\alpha) &= 1. \end{aligned}$$

Darboux's Theorem says that every contact form is locally isomorphic to the standard contact form on \mathbb{R}^3 :

$$\alpha_0 = dz + xdy.$$

Thus, only the global properties of contact manifolds are of interest. To organize the study of global properties, Eliashberg divided contact structures on 3-manifolds into two classes: **overtwisted**, which contain an embedded disk D that is tangent to ξ along ∂D , and **tight**, which do not. Eliashberg proved that overtwisted structures are classified up to contact isotopy by the homotopy class of their underlying 2-plane fields [6]. Tight structures are more rigid, as evidenced, for example, by the existence of a unique tight contact structure on S^3 [8], by the existence of a manifold that does not admit a tight structure [14], and by the Bennequin inequality (see below).

One effective way to study global properties of contact manifolds is to look at the Legendrian knots they support. A **Legendrian knot** is an embedded circle $L \subset M$ that is always tangent to ξ . An ambient isotopy of L through other Legendrian knots is a **Legendrian isotopy**. Note that Legendrian knots are plentiful; for example, any smooth knot can be continuously approximated by a Legendrian knot.

As mentioned in the introduction, there are two "classical" invariants for null-homologous Legendrian knots up to Legendrian isotopy. The first classical invariant is the **Thurston-Bennequin number** $tb(L)$, which measures the twisting of the contact planes around the knot L . More precisely, let \hat{L} result from pushing L out a small distance along a vector field that is transverse to ξ along L . Define $tb(L)$ to be the linking number of L and \hat{L} . The second classical invariant, the **rotation number**, is defined for *oriented* Legendrian knots. It measures the twisting of the tangent direction to L inside ξ . More precisely, let Σ be a Seifert surface for L . This means that $\partial\Sigma = L$, so $[\Sigma]$ is a class in $H_2(M, L; \mathbb{Z})$. Trivialize ξ over Σ ; then $r(L; [\Sigma])$ is the winding number of the oriented tangent direction to L with respect to this trivialization. In a tight contact manifold, the classical invariants are restricted by the Bennequin inequality, which was originally proved by Bennequin [3] and generalized by Eliashberg [9] to:

$$tb(L) + |r(L; [\Sigma])| \leq -\chi(\Sigma).$$

The contact manifolds of interest in this paper are circle bundles E over closed Riemann surfaces F with contact structures transverse to the fibers. So long as the Euler number $e(E)$ is negative, Giroux [19] and Honda [20] proved that such contact structures exist, are tight, and are unique up

to contact isotopy.⁴ If, in addition, the contact structure is invariant along the fibers, the Lutz [21] proved that it is unique up to equivariant contactomorphism.

The following construction of the unique invariant contact structure transverse to the fibers of $E \xrightarrow{\pi} F$ will be used throughout this paper. Let $\mathcal{E} \xrightarrow{\pi} F$ be a Hermitian line bundle and let E be its unit circle bundle. Let α be the restriction of a unitary connection form on \mathcal{E} to E . Thus, the curvature $\Omega \in \Omega^2(F)$ is given by:

$$(1) \quad \pi^*\Omega = id\alpha.$$

The connection form is a positive contact form if and only if its curvature is strictly negative. It follows that $e(E) < 0$. The Reeb field for α points along the fibers. Note that E is holomorphically filled by the unit disk bundle of \mathcal{E} , so it is tight [7].

Definition 2.1. A **contact circle bundle** is a circle bundle $E \xrightarrow{\pi} F$ together with a contact form α as described above.

The standard contact S^3 is the simplest example of a contact circle bundle. Consider S^3 to be the unit sphere inside \mathbb{C}^2 . Let ξ_0 be the 2-plane field defined by the complex tangencies to S^3 . It is straightforward to check that ξ_0 is the kernel of the form

$$\alpha_0 = \frac{1}{2} \sum_{j=1,2} x_j dy_j - y_j dx_j.$$

The Reeb field of α_0 generates the Hopf fibration.

Note that the standard structure on S^3 is an example of this construction. For a more detailed introduction to contact geometry, see [1, 12, 17].

2.2. Diagrams of Legendrian Knots. This section explains how a Legendrian knot L in a contact circle bundle can be described combinatorially by three pieces of data: its projection $\pi(L)$ to the base F , a choice of Reeb chord above every double point of $\pi(L)$, and an integer vector with one component for each region of $F \setminus \pi(L)$. The last two characterize the interaction of L with the topology of E in a similar manner to Turaev's shadow link representation for topological knots in circle bundles [25].

Recall that the Reeb flow goes around the fibers of E . Thus, as mentioned in Section 1.2, above a double point of $\pi(L)$, there exist countably many isolated Reeb chords that start and end on different strands. These come from concatenating a short chord between the strands with a chord that winds several times around the fiber. Above each double point, choose one of the two Reeb chords with distinct endpoints and with minimum length among all chords with the same endpoints. Display this choice on $\pi(L)$ as follows: in each quadrant near a double point, the orientation of F gives a counter-clockwise orientation to the edges of $\pi(L)$ that bound the quadrant; see Figure 2. If the starting point of the chosen Reeb chord lies on the incoming strand, then decorate the quadrant with a $+$. Otherwise, leave it blank. After following this algorithm, each double point has two opposing quadrants decorated with a $+$. Refer to this decorated diagram as $\pi(L)^+$.

The next step is to quantize the holonomy of α over the piecewise smooth boundary of a surface immersed in F . Of particular interest in this section will be the regions of the graph $\pi(L) \subset F$; later on, the definition of the invariant will require the consideration of immersed disks.

Let Σ be an oriented surface with non-empty boundary and let $\{z_1, \dots, z_m\}$ be marked points on $\partial\Sigma$. Let $f : \Sigma \rightarrow F$ be an orientation-preserving immersion on the interior of Σ . Assume that f extends smoothly to $\partial\Sigma$ away from the marked points and that f maps each marked point to a

⁴The existence result is really a consequence of the ‘‘Milnor-Wood’’ inequalities for contact structures; see [12, 19, 23].

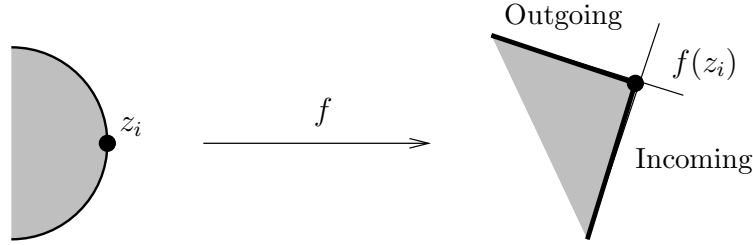


FIGURE 1. The map f sends a marked point z_i to a double point.

double point of $\pi(L)$. At a marked point, $f|_{\partial\Sigma}$ can turn from one strand above the double point to another, as in Figure 1(a). With respect to the orientation on $\partial\Sigma$, say that $f|_{\partial\Sigma}$ passes from the **incoming strand** to the **outgoing strand**.

Above each $f(z_i)$, let x_i Reeb chord with distinct endpoints. Let $l(x_i)$ be the length of x_i ; assume that $0 < l(x_i) < 2\pi$.⁵ Define the number ϵ_i as follows:

$$(2) \quad \epsilon_i = \begin{cases} +1 & x_i \text{ flows from the incoming to the outgoing strand,} \\ -1 & \text{otherwise.} \end{cases}$$

Definition 2.2. Let the immersion f and the chords x_1, \dots, x_m be defined as above. The **defect** of f with respect to x_1, \dots, x_m is the integer defined by:

$$(3) \quad n(f; x_1, \dots, x_m) = \frac{1}{2\pi} \left(\int_{\Sigma} f^* \Omega + \sum_{j=1}^m \epsilon_j l(x_j) \right).$$

Extend the defect linearly to formal chains of immersions.

Here is another description of the defect. Suppose that $\partial\Sigma$ is connected. Choose the component of $\partial\Sigma \setminus \{z_1, \dots, z_m\}$ that lies between z_1 and z_2 and lift it to a Legendrian curve in f^*E . Start lifting the next component at a length $\epsilon_2 l(x_2)$ along the fiber away from the end of the first lift. Proceed this way until all components of $\partial\Sigma \setminus \{z_1, \dots, z_m\}$ have been lifted. The defect is the winding number around the fiber of the curve defined by the lifted path together with the Reeb chords; in other words, the defect is a coarse measure of the holonomy of the connection α above the curve $f(\partial\Sigma)$. This construction justifies the assertion that the defect is an integer.

As a final note on the defect, suppose that $\epsilon_i = +1$ for n of the m chords. Since the curvature of α is strictly negative and the Reeb chords have length less than 2π , the following holds:

Lemma 2.3. *The defect is bounded above by $n - 1$.*

Now it is time to put all of this information together in a diagram. The information about the defects of the regions of $F \setminus \pi(L)$ is recorded in an integer vector $\vec{n}(L)$ that has one component n_i for each region R_i of $\pi(L)$. If the boundary of R_i contains the double points under the previously chosen Reeb chords x_1, \dots, x_m , then the components of $\vec{n}(L)$ are defined by:

$$(4) \quad n_i = n(R_i; x_1, \dots, x_m).$$

Note that the signs ϵ_j are positive if R_i covers a quadrant with a $+$ at $\pi(x_j)$ and negative otherwise.

⁵This length may be defined either in terms of the Hermitian metric on \mathcal{E} or, more topologically, by $\int_{x_i} \alpha$.

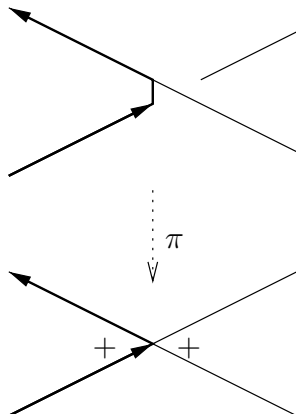


FIGURE 2. The representation of a choice of chord above a double point.

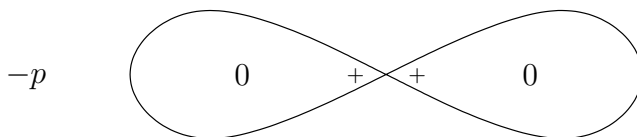


FIGURE 3. The diagram of a local Legendrian unknot in $L(p, 1)$.

Definition 2.4. Let L be a Legendrian knot in a contact circle bundle (E, α) with chosen Reeb chords over each double point of $\pi(L)$. A pair (Γ^+, \vec{n}) , where Γ^+ is a circle immersed in F together with $+$ decorations at its double points and \vec{n} is an integer vector with one component for each region of $F \setminus \Gamma$, is a **diagram** for L if there exists an orientation-preserving diffeomorphism ϕ of F that satisfies:

1. $\phi(\Gamma) = \pi(L)$,
2. ϕ sends quadrants near double points of Γ labeled with a $+$ to such quadrants in $\pi(L)$, and
3. $\vec{n} = \vec{n}(L)$.

The immersed circle Γ will frequently be viewed as a 4-valent graph in F . The components of the vector \vec{n} are restricted by the following easy consequence of the definition of the defect and of the Chern-Weil theorem:

Proposition 2.5. *Let (Γ^+, \vec{n}) be the diagram of a Legendrian knot in $E \rightarrow F$. Then:*

$$\sum_i n_i = e(E).$$

Example. The projection of a small, null-homologous unknot in the lens space $L(p, 1)$ with $tb = -1$ to S^2 is given by the Whitney immersion; see Figure 3. Choose the shorter of the two Reeb chords at the crossing. The components of \vec{n} associated with the two lobes of the immersion are both 0. By Proposition 2.5, the defect for the remaining region must be $-p$.

Example. The knot K pictured in Figure 4 is topologically equivalent to the Whitehead double of a fiber of $L(p, 1)$ over a point in S^2 .

As in Section 8 of Chekanov's paper [5], it is possible to combinatorially characterize Legendrian knot diagrams when $F \simeq S^2$. In order to specify which pairs (Γ^+, \vec{n}) are diagrams for Legendrian

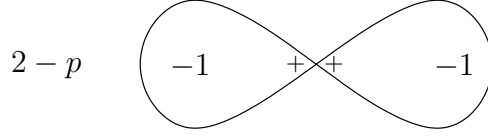


FIGURE 4. The diagram of the Whitehead double of a fiber of $L(p, 1)$.

knots, some notation is necessary. Think of Γ as a 4-valent graph with vertices p_1, \dots, p_r and regions U_1, \dots, U_{r+2} in $F \setminus \Gamma$. Following Chekanov, define two vector spaces over \mathbb{R} : Q_Γ is generated by the vertices p_j , and V_Γ is generated by the regions U_j . The Euler number e of $E \rightarrow S^2$ generates a hyperplane in V_Γ :

$$(5) \quad V_{\Gamma, e} = \left\{ \sum_i c_i U_i \in V_\Gamma \mid \sum_i c_i = 2\pi e(E) \right\}.$$

Let $U_+^1(p_j)$ and $U_+^2(p_j)$ be the two regions that are decorated with a $+$ near p_j . Let $U_-^1(p_j)$ and $U_-^2(p_j)$ be the other two regions. Define a linear map $\Psi : Q_\Gamma \rightarrow V_\Gamma$ by:

$$(6) \quad \Psi(p_j) = U_+^1(p_j) + U_+^2(p_j) - U_-^1(p_j) - U_-^2(p_j).$$

Properly combined, these spaces and maps characterize diagrams of Legendrian knots in E :

Proposition 2.6. *Let $Q_\Gamma^{>0}$ be the vectors in Q_Γ with all positive components, and let $V_{\Gamma, e}^{<0}$ be the vectors in $V_{\Gamma, e}$ with all negative components. Then (Γ^+, \vec{n}) is the diagram of a Legendrian knot in $E \rightarrow S^2$ if and only if*

$$(7) \quad \Psi(Q_\Gamma^{>0}) \cap (2\pi\vec{n} - V_{\Gamma, e}^{<0}) \neq \emptyset.$$

Proof. First suppose that (Γ^+, \vec{n}) is the diagram of a Legendrian knot L . Let $\phi \in \text{Diff}^+(S^2)$ have the property that $\phi(\Gamma^+) = \pi(L)^+$. Let x_j be the chosen Reeb chord at the vertex p_j . Define $q_L \in Q_\Gamma$ by:

$$q_L = \sum_j l(x_j) p_j.$$

Clearly, $q_L \in Q_\Gamma^{>0}$. Similarly, define an element $v_\phi \in V_\Gamma$ by:

$$v_\phi = \sum_j k_j U_j,$$

where $k_j = \int_{U_j} \Omega$, the total curvature of α over U_j . By Proposition 2.5 and the fact that the curvature is strictly negative, $v_\phi \in V_{\Gamma, e}^{<0}$. Thus, by the definition of the defect,

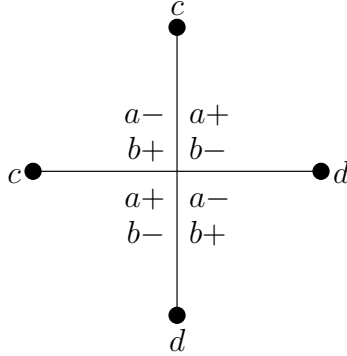
$$\Psi(q_L) = 2\pi\vec{n} - v_\phi.$$

The first half of the proposition follows.

Conversely, suppose that there exist elements $q \in Q_\Gamma^{>0}$ and $v \in V_{\Gamma, e}^{<0}$ that satisfy

$$(8) \quad \Psi(q) = 2\pi\vec{n} - v.$$

On one hand, it is not hard to construct $\phi \in \text{Diff}^+(S^2)$ so that $v = v_\phi$. It remains to show that Legendrian curve L that projects to $\phi(\Gamma^+)$ is actually a knot. To do this, it suffices to show that the total holonomy around $\phi(\Gamma)$ is an integral multiple of 2π .

FIGURE 5. Labels at a double point of Γ .

To measure the holonomy, orient Γ and let $\{C_1, \dots, C_m\}$ be the Seifert circles of Γ .⁶ Each C_i bounds a disk D_i with corners; let k_i be the total curvature over D_i and let n_i be the defect of D_i for the Reeb chords chosen by the “+” decorations on Γ^+ . Note that if D_i covers several regions, the defect and the total curvature of D_i are the sum of the defects or curvatures, respectively, of those regions. The holonomy around a lift of $\phi(\Gamma)$ is the sum of the k_i , counted with sign: if Γ goes around ∂D_i counter-clockwise, then D_i contributes k_i to the holonomy; otherwise, D_i contributes $-k_i$.

Equation (8) implies that $k_i = 2\pi n_i - \sum_j \epsilon_j q_j$, where the q_j are summed over all corners of D_i . It is not hard to see that the $\epsilon_j q_j$ cancel out in the signed sum of the curvatures k_i .

It follows that $\sum_i \pm k_i = \sum_i \pm 2\pi n_i$. Since the n_i are integers this proves the proposition. \square

3. A COMBINATORIAL DEFINITION OF THE INVARIANT

There are three building blocks of the invariant promised in Theorem 1.1. The first is a graded filtered algebra \mathcal{A} associated to a knot diagram. The second is a differential on the algebra that, roughly speaking, counts immersed disks with boundary in the knot diagram. The last building block is an algebraic equivalence relation on the DGAs whose equivalence classes are invariant under Legendrian isotopy. This section considers each building block in turn.

3.1. The Underlying Algebra \mathcal{A} .

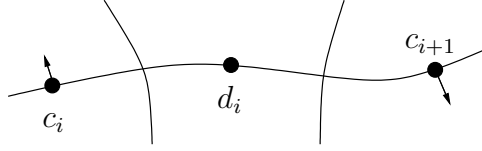
3.1.1. Generators for the Algebra. Let (Γ^+, \vec{n}) be a diagram for a Legendrian knot L . The definition of the generators of \mathcal{A} requires a few additional decorations on the diagram. Number the double points from 1 to m . To the double point labeled i , associate two countable sets of generators $\{a_i^k\}_{k=0,1,\dots}$ and $\{b_i^k\}_{k=0,1,\dots}$. In addition, label the quadrants around each double point as in Figure 5.⁷

On the interior of each edge e of Γ , choose a point \hat{e} . Number these edge points from 1 to $2m$ by traversing Γ , starting from an arbitrary edge. To the edge point \hat{e}_{2i-1} , associate a countable set of generators $\{c_i^k\}_{k=1,2,\dots}$. Similarly, to the edge point \hat{e}_{2i} , associate a countable set of generators $\{d_i^k\}_{k=1,2,\dots}$. Hereafter, the edge points \hat{e}_{2i-1} will be referred to as c_i , and the edge points \hat{e}_{2i} will be referred to as d_i . Further, choose a direction transverse to Γ at each c_i ; see Figure 6.

Definition 3.1. The **special points** of Γ consist of the edge points \hat{e} and the double points.

⁶This is where the assumption that $F \simeq S^2$ is necessary. More generally, this proof works for knots with null-homologous projections in any base F .

⁷These labels play the same role as the \pm labels in the Chekanov-Eliashberg differential.

FIGURE 6. Decorations at the edge points of Γ .

Definition 3.2. Let $\mathcal{A}_{(\Gamma^+, \vec{n})}$ be the filtered unital based⁸ associative algebra with coefficients in \mathbb{Z}_2 freely generated by the letters a_i^k , b_i^k , $c_i^{k'}$, and $d_i^{k'}$ for $i = 1, \dots, m$, $k = 0, 1, 2, \dots$, and $k' = 1, 2, 3, \dots$. The subscript (Γ^+, \vec{n}) will be dropped if there is no danger of confusion.

The k^{th} level of the filtration $F^0 \mathcal{A} \subset F^1 \mathcal{A} \subset \dots$ is generated as a vector space by the monomials

$$(9) \quad \left\{ x_1^{j_1} \cdots x_m^{j_m} \in \mathcal{A} \mid \sum_i j_i \leq k \right\}.$$

Remark. Recall that there are two types of Reeb chords for a Legendrian knot $L \subset E$:

1. Those that start and end on different strands. As mentioned in Section 2.2, over a double point of $\pi(L)$, there are countably many such isolated Reeb chords, indexed by their “winding number” around the fiber.
2. Those that begin and end at the same point on L . There are countably many of them over any given point of L , indexed by their “winding number” around the fiber.

Assume that $\Gamma = \pi(L)$. The generators a_i^k and b_i^k of $\mathcal{A}_{(\Gamma^+, \vec{n})}$ correspond to the first type of Reeb chord that project to the double point i , wind around the fiber k times, and whose endpoints lie on different strands of L above the double point. The chord corresponding to the a_i^0 (respectively, b_i^0) generator is the one that passes from the incoming to the outgoing strand when the boundary of the quadrant labeled a_i+ (resp. b_i+) is given a counter-clockwise orientation.

By definition, the **length** l of these generators is

$$(10) \quad \begin{aligned} l(a_i^k) &= l(a_i^0) + 2\pi k, \\ l(b_i^k) &= l(b_i^0) + 2\pi k. \end{aligned}$$

The generators c_i^k and d_i^k represent the Reeb chords that start and end at the same point and project to the points labeled c_i and d_i , respectively. Note that

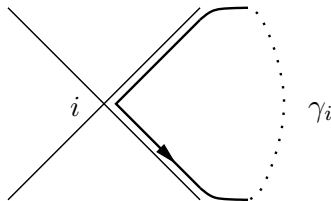
$$(11) \quad l(c_i^k) = l(d_i^k) = 2\pi k.$$

Instead of working directly with the algebra \mathcal{A} , it will sometimes be useful to organize the generators into power series in $\mathcal{A}[[T]]$. Of course, all equations involving these power series should be understood as a sequence of equations relating the coefficients of T^k on the left hand side to those on the right hand side for each k . To formalize the power series idea, define:

Definition 3.3. A filtered unital based associative algebra \mathcal{A} is **generated by power series** if the chosen generators of \mathcal{A} may be grouped into sequences $\{x_i^j\}_{j \geq k_i}$, where $x_i^j \in F^j \mathcal{A}$. For short, say that \mathcal{A} is generated by the power series

$$\mathbf{x}_i = \sum_{j=k_i}^{\infty} x_i^j T^j, \quad i = 1, \dots, m.$$

⁸A based algebra is an algebra together with a choice of generating set.


 FIGURE 7. Combinatorial construction of the capping path γ_i .

Remark. So long as there is a universal bound on the number of generators in each level of the filtration, the algebra may be generated by power series.

The generating power series of $\mathcal{A}_{(\Gamma^+, \vec{n})}$ are:

$$\begin{aligned} \mathbf{a}_i &= \sum_{k=0}^{\infty} a_i^k T^k & \mathbf{b}_i &= \sum_{k=0}^{\infty} b_i^k T^k \\ \mathbf{c}_i &= \sum_{k=1}^{\infty} c_i^k T^k & \mathbf{d}_i &= \sum_{k=1}^{\infty} d_i^k T^k \end{aligned}$$

Note that, since the power series \mathbf{c}_i starts in degree one, the element $1 + \mathbf{c}_i$ is invertible in $\mathcal{A}[[T]]$.

3.1.2. *Grading.* A generator of $\mathcal{A}_{(\Gamma^+, \vec{n})}$ has a grading if it is associated to an edge point or to a double point that satisfies an additional geometric condition. Define a **capping path** γ_i for the double point i to be one of the two oriented paths in Γ that begin at i , run along Γ until they first return to i , and induce a counter-clockwise orientation on the quadrant they bound near i ; see Figure 7.

There are two quantities associated to a *contractible* capping path γ_i : its holonomy and its rotation. To define the holonomy, assume that the quadrant that γ_i bounds has an $a+$ label (see Figure 5); the following constructions are analogous if there is a $b+$ label. In the former case, say that γ_i is a **capping path for a_i** ; in the latter, say that γ_i is a **capping path for b_i** . Using the standard Seifert Circle algorithm, construct a chain of embedded surfaces Σ_i with $\partial\Sigma_i = \gamma_i$. With this in hand, define the holonomy k_i of the capping path by:

$$(12) \quad k_i = -n(\Sigma_i; a_i).$$

Note that k_i may be computed by summing up (with sign) the defects listed in \vec{n} of the embedded surfaces that comprise Σ_i .

To define the rotation, note that the contractibility assumption implies that $\gamma_i \subset D^2 \subset F$ for some embedded disk D^2 in F . The rotation number of γ_i with respect to a trivialization of TD^2 may be computed as the fractional number of counter-clockwise rotations made by the tangent vector to γ_i .⁹ Call this number $r_D(\gamma_i)$. If $\Sigma_i \subset D^2$, then the trivialization of TD^2 induces one on $T\Sigma_i$. In general, however, Σ_i may not lie inside the disk, and corrections to the trivialization must be made. If p is some point in F outside the disk, then the **rotation number** of γ_i is:

$$r(\gamma_i) = r_D(\gamma_i) + \chi(F)(p \cdot \Sigma_i).$$

⁹In practice, this trivialization will be given by the presentation of the diagram.

Definition 3.4. Without loss of generality, assume that the strands of Γ meet orthogonally at i . Suppose that a_i has a contractible capping path. The grading of $a_i^{-n(\gamma_i; a_i)}$ is a number in $\frac{1}{e(E)}\mathbb{Z}$ defined by:

$$(13) \quad |a_i^{-n(\gamma_i; a_i)}| = 2r(\gamma_i) - \frac{1}{2}.$$

Let $\mu_E = -\frac{\chi(F)}{e(E)}$. For arbitrary $k = 0, 1, 2, \dots$, define:

$$(14) \quad \begin{aligned} |a_i^k| &= |a_i^{-n(\gamma_{a_i}; a_i)}| + (k + n(\gamma_{a_i}; a_i)) 2\mu_E, \\ |b_i^k| &= 2\mu_E(2k + 1) - 1 - |a_i^k|. \end{aligned}$$

Furthermore, the generators c_j^k and d_j^k are graded as follows:

$$(15) \quad \begin{aligned} |c_j^k| &= 2k\mu_E, \\ |d_j^k| &= 2k\mu_E - 1. \end{aligned}$$

The grading is well-defined up to the choice of capping path. If Γ is contractible in F , then there are many possible choices. Any two capping paths will differ by a path that traverses the entire knot an integral number of times. If $n(L)$ is the total holonomy around the knot, traversing the knot will add $2r(L)$ to the rotation of γ_i and $n(L)$ to $n(\gamma_i; a_i)$. Thus:

Proposition 3.5. *For a knot whose projection is contractible, the grading on \mathcal{A} in Definition 3.4 is well-defined modulo $2r(L) + 2\mu_E n(L)$.*

Note that this reduces to the ambiguity of Chekanov's grading in [5] when L is null-homotopic in E .

Remark. This grading is a combinatorial translation of the Conley-Zehnder index of a Reeb chord. Note that μ_E is the Maslov index of a fiber. See [11] or [16] for a more geometric construction.

3.2. The Differential on \mathcal{A} . The differential on \mathcal{A} is the sum of two parts: an “external” differential and an “internal” differential. This is analogous to the differential in Morse-Bott theory, which splits into flowlines *between* critical submanifolds and flowlines *inside* the critical submanifolds. Since the definitions of the internal and external differentials are somewhat involved, a simple example is calculated in Section 3.3.

3.2.1. The External Differential. The external differential ∂_{ext} is defined in much the same way as the Chekanov-Eliashberg differential [5, 16]: it is a count of certain immersed disks in F with boundary in the diagram Γ . There are, however, several new features that change the nature of the boundary conditions for the disks. First of all, there are now many generators associated to each double point. Secondly, there are new generators associated to the edge points. Lastly, the topology of the bundle, as recorded by the defect, must be taken into account.

The first step is to define appropriate spaces of immersions of marked disks. In this context, a **marked disk** is a disk D^2 together with $m + 1$ distinct marked points z, w_1, \dots, w_m , arranged counter-clockwise on ∂D^2 . Let x be a label in the set $\{a_i, b_i, d_i\}_{i=1\dots n}$ and let y_1, \dots, y_m be labels in the set $\{a_i, b_i, c_i\}_{i=1\dots n}$.

Definition 3.6. The **space of immersed marked disks** $\Delta(x; y_1, \dots, y_m)$ consists of orientation-preserving immersions of marked disks $f : D^2 \rightarrow F$ that satisfy:

1. The map f sends ∂D^2 to Γ and is smooth off of the marked points. The restriction of f to ∂D^2 is an immersion off of the marked points.
2. The map f sends z to x and w_j to y_j .

3. Near each marked point whose image is a double point, the image of f in a neighborhood of the marked point covers but one quadrant of Γ . If x is a double point, then f covers one of the two quadrants labeled $x+$; say that f has a **positive corner** at x . If y_j is a double point, then f covers a quadrant labeled y_j- ; say that f has a **negative corner** at y_j .
4. If $f|_{\partial D^2}$ crosses an edge point labeled c_i , then that c_i must be the image of a marked point.

Two immersions f and g are equivalent in Δ if there exists a smooth automorphism ϕ of the marked disk so that $f = g \circ \phi$.

Using these spaces, the exterior differential of each generator of \mathcal{A} may be defined via power series formulae.

Definition 3.7. Let x, y_1, \dots, y_m be as above. Let $n(f; x, y_1, \dots, y_m)$ be the defect of f . The **exterior differential** ∂_{ext} is defined by the formula:

$$(16) \quad \partial_{ext} \mathbf{x} = \sum_{(y_1, \dots, y_m)} \sum_{f \in \Delta(x; y_1, \dots, y_m)} \tilde{\mathbf{y}}_1 \cdots \tilde{\mathbf{y}}_m T^{-n(f; x, y_1, \dots, y_m)},$$

where

$$\tilde{\mathbf{y}} = \begin{cases} 1 + \mathbf{y} & y = c_j \text{ and the transversal at } c_j \text{ points into } \text{Im } f; \\ (1 + \mathbf{y})^{-1} & y = c_j \text{ and the transversal at } c_j \text{ points out of } \text{Im } f; \\ \mathbf{y} & \text{otherwise.} \end{cases}$$

If $m = 0$, then the contribution of $\Delta(x)$ is 1 for every distinct element of $\Delta(x)$.

Extend ∂_{ext} to all of \mathcal{A} via the Leibniz rule.

Remark. Strictly speaking, the defect of an element of $\Delta(x; y_1, \dots, y_m)$ is a slight abuse of notation since x or some of the y_i may lie on an edge rather than at a double point. Such chords are ignored in the calculation of the defect.

The defect of an element f of $\Delta(x; y_1, \dots, y_m)$ may be easily computed combinatorially. Let \tilde{n} be the defect of f computed with respect to the choice of chords given by the diagram Γ^+ , i.e. add up the defects in \tilde{n} of the regions of Γ that lie in the image of f . The defect of f with respect to the chords x, y_1, \dots, y_m comes from making the following adjustments to \tilde{n} :

1. If x is a double point label and the $+$ decoration from Γ^+ does not lie in the same quadrant as the label $x+$, then add 1 to \tilde{n} .
2. For $i = 1, \dots, m$, if y_i is a double point label and the $+$ decoration lies in the same quadrant as the label y_i- , then subtract 1 from \tilde{n} .

The result is $n(f; x, y_1, \dots, y_m)$.

Proposition 3.8. *The exterior differential is well-defined. In particular, each coefficient in equation (16) is given by a finite sum.*

Proof. Fix $k \geq 0$ and let $y_1^{k_1} \cdots y_m^{k_m}$ be a term in the differential of x^k coming from a map $f \in \Delta(x; y_1, \dots, y_m)$. Equation (16) implies:

$$(17) \quad k + n(f; x, y_1, \dots, y_m) = \sum_{j=1}^m k_j,$$

and hence there are finitely many choices for the k_j .

It now suffices to prove that, up to equivalence, the sets $\Delta(x; y_1, \dots, y_m)$ are finite. Suppose that Γ coincides with $\pi(L)$. In this situation, the defining equation for the defect (see Definitions 2.2

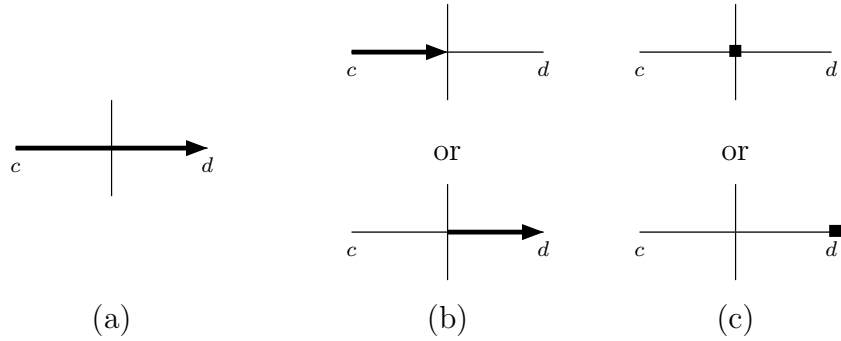


FIGURE 8. (a) A flowline. (b) Half flowlines. (c) Vertex flowlines.

and 2.4) is:

$$(18) \quad n(f; x, y_1, \dots, y_m) = \frac{1}{2\pi} \left(\int_D f^* \Omega + l(x^0) - \sum_{j=1}^m l(y_j^0) \right).$$

Here, it is understood that $l(c^0) = l(d^0) = 0$. The terms $l(y_j^0)$ are understood to be 0 if y_j is a c_j generator, and similarly for $l(x^0)$. Using the fact that the curvature Ω is strictly negative and that $l(x^k) = l(x^0) + 2\pi k$, equations (17) and (18) lead to:

Lemma 3.9.

$$(19) \quad 0 > \int_D f^* \Omega \geq -l(x^k) + \sum_{j=1}^m l(y_j^k).$$

In particular, the total curvature of the regions of $\pi(L)$ covered by f is bounded below by $-l(x^k)$. This is a uniform bound for any map f that contributes to $\partial_{ext} x^k$. Thus, there exists a bound on the number of regions that f covers, and hence there exist finitely many possible maps f . \square

Remark. Proposition 3.8 does *not* imply that the sum in (16) is finite; it merely shows that it is well-defined as a power series.

3.2.2. The Internal Differential. To define the internal differential ∂_{int} , it helps to think of Γ as having a ‘‘Morse function’’ with its maxima at the c_i and its minima at the d_i . Schematically, the internal differential is defined by counting the flowlines, the ‘‘half-flowlines’’ between the extrema and the crossings, and ‘‘vertex flowlines’’ that stay fixed at the crossings and the minima. See Figure 8.

Definition 3.10. Let the labels near a double point be as in Figure 9(a) and near a point labeled with a c as in Figure 9(b). The **internal differential** ∂_{int} is given by:

For a: The internal differential comes from the two half-flowlines that start at the double point and end at the adjacent d points:

$$\partial_{int} \mathbf{a} = \mathbf{ad}' + \mathbf{da}.$$

For b: The first two terms come from the two half-flowlines that start at the double point and end at the adjacent d points; the last comes from a vertex flowline at the double point:

$$\partial_{int} \mathbf{b} = \mathbf{bd} + \mathbf{d}'\mathbf{b} + \mathbf{bab}T.$$

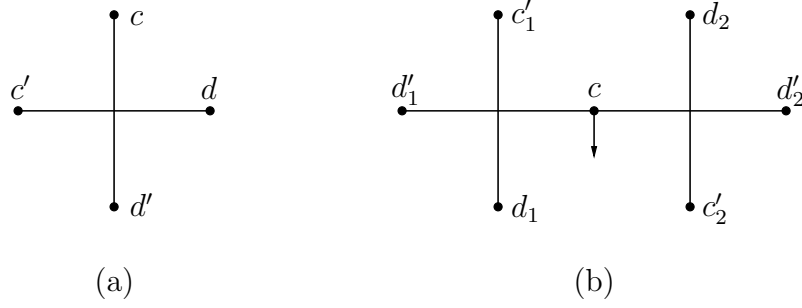


FIGURE 9. (a) The configuration for a and b in Definition 3.10. (b) The configuration for the differential of c in Definition 3.10.

For c : The first set of terms comes from the flowline and the half-flowline that depart c to the left in Figure 9(b). The second set comes from a flowline and the half-flowline that go to the right:

$$\partial_{int} \mathbf{c} = (1 + \mathbf{c})(\mathbf{d}'_1 + \mathbf{b}_1 \mathbf{a}_1 T) + (\mathbf{d}'_2 + \mathbf{b}_2 \mathbf{a}_2 T)(1 + \mathbf{c}).$$

If the relative positions of the c'_1 and d_1 on the vertical strand at the left of Figure 9(b) are reversed, then $\mathbf{b}_1 \mathbf{a}_1 T$ becomes $\mathbf{a}_1 \mathbf{b}_1 T$, and similarly for the c'_2 and d_2 .

For d : The internal differential comes from a vertex flowline at d :

$$\partial_{int} \mathbf{d} = \mathbf{d} \mathbf{d}.$$

Extend ∂_{int} to all of \mathcal{A} via the Leibniz rule.

3.2.3. The Full Differential. The internal and external differentials combine to form the full differential on \mathcal{A} :

Theorem 3.11. *The full differential $\partial = \partial_{int} + \partial_{ext}$ on \mathcal{A} satisfies $\partial \circ \partial = 0$. Further, ∂ preserves the filtration on \mathcal{A} and, when the grading is defined as in Section 3.1.2, has degree -1 .*

The proof that $\partial \circ \partial = 0$ will be delayed until Section 5.

Proof that ∂ preserves filtration. Suppose that $\mathbf{y}_1 \cdots \mathbf{y}_m T^l$ is a term in $\partial \mathbf{x}$. Expanding, this gives the terms $y_1^{j_1} \cdots y_m^{j_m}$ in ∂x^k for $k = l + \sum k_j$. So long as $l \geq 0$, ∂ preserves filtration.

For ∂_{int} , $l \geq 0$ by inspection. For ∂_{ext} , Lemma 2.3 and the fact that the disks that contribute to ∂_{ext} have but one positive corner imply that $l \geq 0$. \square

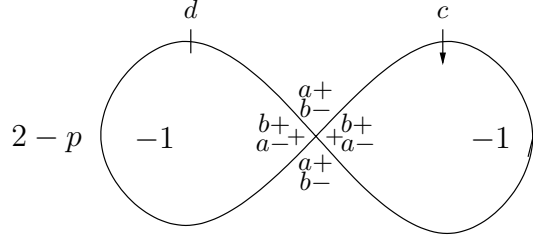
Proof that ∂ has degree -1 . For the internal differential, the theorem follows from direct calculations. For example, consider the internal differential of a^k :

$$\partial_{int} a^k = \sum_{j=0}^{k-1} a^j d^{k-j} + d^{k-j} a^j.$$

On the left hand side, the grading is:

$$\begin{aligned} |a^k| &= |a^j| + 2\mu_E(k-j) \\ &= |a^j| + |d^{k-j}| + 1. \end{aligned}$$

This is one more than the grading of the terms on the right hand side. The other computations using Definition 3.4 are similar.

FIGURE 10. The labeling of the diagram of the knot $L \subset L(p, 1)$.

For the external differential, suppose that $y_1^{k_1} \cdots y_m^{k_m}$ is an arbitrary term in $\partial_{ext} x^k$ that comes from a disk f . Let γ_x be the capping path for x , and γ_i be the capping path for y_i , as defined in Section 3.1.2. Note that if the algorithm produces a capping path for a_i , then the same gradings are produced if $-\gamma_{a_i}$ is used as a capping path for b_i . For c_i and d_i , define the capping path to be the constant path. Define $r(\gamma_{c_i}) = 0$ and $n(\gamma_{c_i}; c_i) = 0$, and similarly for d_i .

Combine the capping paths of the generators x, y_1, \dots, y_m with $f|_{\partial D}$ to form a loop:

$$\gamma = \text{Im } f|_{\partial D} \sqcup -\gamma_x \sqcup \gamma_1 \sqcup \cdots \sqcup \gamma_m.$$

Since γ is a smooth closed curve in Γ , either

$$(20) \quad 2r(\gamma) + 2\mu_E n(\gamma) \equiv 0 \pmod{\mu(L)}$$

if Γ is contractible in F , or γ itself must be contractible in F , so:

$$(21) \quad r(\gamma) = 0.$$

On the other hand, it is possible to calculate $2r(\gamma) + 2\mu_E n(\gamma)$ piece by piece:

$$(22) \quad \begin{aligned} r(\gamma) &= r(\text{Im } f|_{\partial D}) - r(\gamma_x) + \sum_{i=1}^m r(\gamma_i), \\ n(\gamma) &= n(f; x, y_1, \dots, y_m) - n(\gamma_x; x) + \sum_{i=1}^m n(\gamma_i; y_i). \end{aligned}$$

Let l be the number of convex corners of f . It is not hard to see that $r(\partial f) = 1 - \frac{l}{4}$. In the case that x is not a d , combining (17) with the equations (22) yields:

$$\begin{aligned} 2r(\gamma) + 2\mu_E n(\gamma) &= 1 - \left(2r(\gamma_x) - \frac{1}{2} + 2\mu_E (n(\gamma_x; x) + k) \right) \\ &\quad + \sum_{y_i \neq c_j} \left(2r(\gamma_i) - \frac{1}{2} + 2\mu_E (n(\gamma_i; y_i) + k_i) \right) + \sum_{y_i = c_j} 2\mu_E k_i \\ &= 1 - |x^k| + \sum_{i=1}^m |y_i^{k_i}|. \end{aligned}$$

The case where $x = d_j$ is entirely similar. The result now follows from (20) or (21). \square

3.3. A Simple Example. Let $L \subset L(p, 1)$ be the knot introduced in the second example of Section 2.2. The labeled diagram (Γ^+, \vec{n}) for L is pictured in Figure 10. The algebra for (Γ^+, \vec{n}) is generated by the power series \mathbf{a} , \mathbf{b} , \mathbf{c} , and \mathbf{d} .

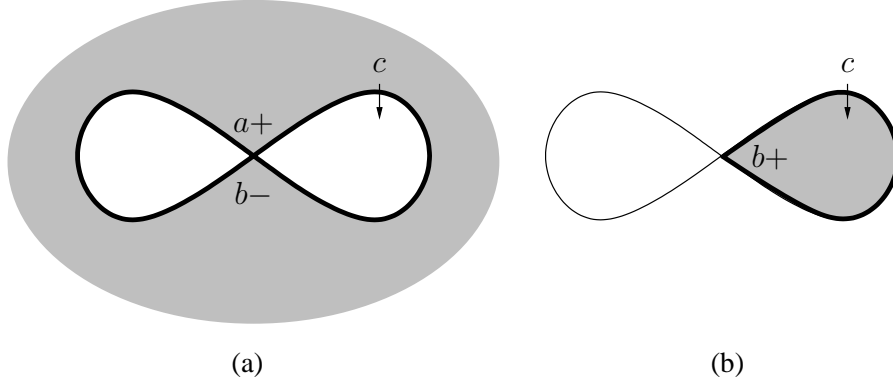


FIGURE 11. (a) The disk giving the term $\mathbf{b}(1 + \mathbf{c})^{-1}T^{p-3}$ in $\partial_{ext}\mathbf{a}$. (b) The disk giving the term $(1 + \mathbf{c})T$ in $\partial_{ext}\mathbf{b}$.

3.3.1. *The Grading.* The curve that runs counter-clockwise around the right-hand lobe of Γ is a capping path for b ; call it γ_b . The rotation number of γ_b is $\frac{3}{4}$ and $n(\gamma_b; b) = -1$, so

$$|b^1| = 2 \cdot \frac{3}{4} - \frac{1}{2} = 1.$$

By (14),

$$\begin{aligned} |a^k| &= \frac{4(k+2)}{p} - 2 & |c^k| &= \frac{4k}{p} \\ |b^k| &= 1 + \frac{4(k-1)}{p} & |d^k| &= \frac{4k}{p} - 1. \end{aligned}$$

Since L is null-homologous and its rotation number is 0, the grading is well-defined in $\frac{1}{p}\mathbb{Z}$.

3.3.2. *The Differential.* Begin with the external differential of \mathbf{a} . The disk f shown in Figure 11(a) contributes one of the two terms of $\partial_{ext}\mathbf{a}$; exchanging the positions of the $a+$ and $b-$ gives the other. By the remark after Definition 3.7, the defect associated to the disk in Figure 11(a) is $3 - p$. Thus,

$$(23) \quad \partial_{ext}\mathbf{a} = \mathbf{b}(1 + \mathbf{c})^{-1}T^{p-3} + (1 + \mathbf{c})^{-1}\mathbf{b}T^{p-3}.$$

Note that the $(1 + \mathbf{c})^{-1}$ factor appears because the transverse direction at c points out of the disk.

The disk shown in Figure 11(b) contributes one of the two terms in $\partial_{ext}\mathbf{b}$. The defect in the diagram is the same as that of the disk, so this gives:

$$(24) \quad \partial_{ext}\mathbf{b} = T + (1 + \mathbf{c})T.$$

The external differential for \mathbf{d} comes from disks whose boundaries pass through d . These are the left-hand lobe of the knot and the disk in Figure 11(a). The defect $n(\cdot; a)$ of the left-hand lobe is one less than the defect in the diagram. The defect of the outer disk agrees with the defect of the diagram. As a result,

$$(25) \quad \partial_{ext}\mathbf{d} = \mathbf{a}T^2 + \mathbf{b}(1 + \mathbf{c})^{-1}\mathbf{b}T^{p-2}.$$

The internal differential is calculated using Definition 3.10 and Figure 9:

$$(26) \quad \begin{aligned} \partial_{int}\mathbf{a} &= \mathbf{ad} + \mathbf{da}, \\ \partial_{int}\mathbf{b} &= \mathbf{bd} + \mathbf{db} + \mathbf{bab}T, \\ \partial_{int}\mathbf{c} &= (1 + \mathbf{c})(\mathbf{d} + \mathbf{ab}T) + (\mathbf{d} + \mathbf{ba}T)(1 + \mathbf{c}), \\ \partial_{int}\mathbf{d} &= \mathbf{dd}. \end{aligned}$$

Equations (23) through (26), together with the fact that $\partial_{ext}\mathbf{c} = 0$, determine the differential ∂ on \mathcal{A} .

3.4. Algebraic Notions. The definition of the DGA in Sections 3.1 and 3.2 depends on the diagram (Γ^+, \vec{n}) , the choice of transverse direction at each c point, and the position of the c and d generators. This section contains the definition of a suitable equivalence relation on the algebras (\mathcal{A}, ∂) which captures how they change with the choices mentioned above.

Before beginning the definitions, some notation is necessary. Throughout this section, “algebra” means “free, unital, graded, based, associative, and filtered algebra”. Any homomorphism of algebras is assumed to respect these properties. The filtration $F^k\mathcal{A}$ is always exhaustive and ascending:

$$(27) \quad \cdots \subset F^k\mathcal{A} \subset F^{k+1}\mathcal{A} \subset \cdots$$

Lastly, generators with filtration k are denoted by x^k when it is convenient to emphasize the filtration.

The building block of the equivalence relation is the “elementary isomorphism”, which are strung together to form “tame isomorphisms”. Let \mathcal{A} and $\bar{\mathcal{A}}$ be algebras with a given correspondence $x \leftrightarrow \bar{x}$ between their generators. Choose a generator $y \in F^k\mathcal{A}$ and an element $u \in F^k\bar{\mathcal{A}}$ so that \bar{y} does not appear in u .

Definition 3.12. The **elementary isomorphism** $\phi_y : \mathcal{A} \rightarrow \bar{\mathcal{A}}$ is defined on the generators by:

$$(28) \quad \phi_y(x) = \begin{cases} \bar{y} + u & x = y, \\ \bar{x} & \text{otherwise.} \end{cases}$$

A **tame isomorphism** is the composition of a (possibly infinite) sequence of elementary isomorphisms $\cdots \circ \phi_{x_2} \circ \phi_{x_1}$ with the property that, for each level k of the filtration, there exists $N_k \in \mathbb{N}$ so that $x_j \notin F^k\mathcal{A}$ for all $j \geq N_k$.

One convenient way to define a tame isomorphism is to use power series. Let \mathcal{A} and $\bar{\mathcal{A}}$ be algebras generated by power series with a given correspondence $\mathbf{x} \leftrightarrow \bar{\mathbf{x}}$ between their generating series. Given a generating series $\mathbf{y} \in \mathcal{A}[[T]]$, let \mathbf{u} be a power series in $\bar{\mathcal{A}}[[T]]$ so that:

1. The coefficient u^k of T^k in \mathbf{u} lies in $F^k\bar{\mathcal{A}}$ for all k ;
2. y^k never appears in u^k .

Lemma 3.13. *The isomorphism $\psi : \mathcal{A}[[T]] \rightarrow \bar{\mathcal{A}}[[T]]$ defined on the generating series by:*

$$(29) \quad \psi(\mathbf{x}) = \begin{cases} \bar{\mathbf{y}} + \mathbf{u} & \mathbf{x} = \mathbf{y}, \\ \bar{\mathbf{x}} & \text{otherwise} \end{cases}$$

gives a tame isomorphism $\psi : \mathcal{A} \rightarrow \bar{\mathcal{A}}$.

Proof. Let ψ_k be the map that sends y^k to $\bar{y}^k + u^k$ and is the identity on all other generators. The first condition above implies that ψ_k is a filtered map. The second condition guarantees that y^k does not appear in u^k . The map ψ is the composition of elementary isomorphisms $\cdots \circ \psi_2 \circ \psi_1 \circ \psi_0$. \square

Remark. Suppose that there is an ordering on the generators of \mathcal{A} that is compatible with the filtration $F^k \mathcal{A}$; for instance, ordering the generators by length in the algebra of a knot. Then, by the same argument as in the proof above, any map ψ defined on the generators by the formula:

$$\psi(x) = x + u_x,$$

where u_x is a term containing only generators that lie strictly below x in the ordering, is a tame isomorphism.

Let \mathcal{E} be an algebra generated by the two power series α and β . Suppose that $|\alpha^k| + 1 = |\beta^k|$, and define

$$(30) \quad \begin{aligned} \partial_{\mathcal{E}} \beta &= \alpha, \\ \partial_{\mathcal{E}} \alpha &= 0. \end{aligned}$$

Definition 3.14. The **stabilization** $S(\mathcal{A}, \partial)$ of a DGA (\mathcal{A}, ∂) is the DGA generated by the union of the generators of \mathcal{A} and those of \mathcal{E} . $S(\mathcal{A}, \partial)$ inherits its grading, filtration, and differential from (\mathcal{A}, ∂) and $(\mathcal{E}, \partial_{\mathcal{E}})$.

Two algebras \mathcal{A} and $\bar{\mathcal{A}}$ are **stable tame isomorphic** if there exist stabilizations S_1, \dots, S_m and $\bar{S}_1, \dots, \bar{S}_n$ and a tame isomorphism:

$$\psi : S_1(\dots S_m(\mathcal{A}) \dots) \rightarrow \bar{S}_1(\dots \bar{S}_n(\bar{\mathcal{A}}) \dots).$$

Two DGAs (\mathcal{A}, ∂) and $(\bar{\mathcal{A}}, \bar{\partial})$ are **stable tame isomorphic** if \mathcal{A} and $\bar{\mathcal{A}}$ are stable tame isomorphic via a chain map intertwining ∂ and $\bar{\partial}$.

Stable tame isomorphism is the appropriate equivalence relation on the DGAs, as evidenced by the following theorem:

Theorem 3.15. *Let L be a Legendrian knot in a contact circle bundle $E \rightarrow F$. Let (\mathcal{A}, ∂) be the DGA for a decorated and labeled diagram of L . The stable tame isomorphism type of \mathcal{A} is:*

1. *Independent of the choice of transverse direction at each c_j ;*
2. *Independent of whether a given edge point has a c_i or d_i label.*
3. *Invariant under Legendrian isotopy of L .*

Notice that $(F^0 \mathcal{A}, \partial)$ is a sub-DGA of the DGA for a knot diagram. Since all of the stable tame isomorphisms involved in Theorem 3.15 preserve the filtration, the following holds:

Corollary 3.16. *The stable tame isomorphism type of the sub-DGA $(F^0 \mathcal{A}, \partial)$ is an invariant of L as in Theorem 3.15.*

Remark. The equivalence relation defined by stable tame isomorphism is stronger than the one defined by quasi-isomorphism; in other words, the homology of (\mathcal{A}, ∂) is also an invariant. To prove this, it suffices to show that the inclusion $i : \mathcal{A} \rightarrow S(\mathcal{A})$ is a chain equivalence on the level of vector spaces. Let $\tau : S(\mathcal{A}) \rightarrow \mathcal{A}$ be the natural projection. Clearly, $\tau \circ i = id_{\mathcal{A}}$. On the other hand, $i \circ \tau$ is chain homotopic to the identity on $S(\mathcal{A})$. To see this, define a vector space map $H : \mathcal{A} \rightarrow S(\mathcal{A})$ by:

$$(31) \quad H(w) = \begin{cases} x\beta^k y & w = x\alpha^k y \text{ and } x \in \mathcal{A}, \\ 0 & \text{otherwise.} \end{cases}$$

It is straightforward to check that H is the required chain homotopy, i.e. that it satisfies:

$$(32) \quad \tau \circ i + Id_{\mathcal{A}} = H \circ \partial + \partial \circ H.$$

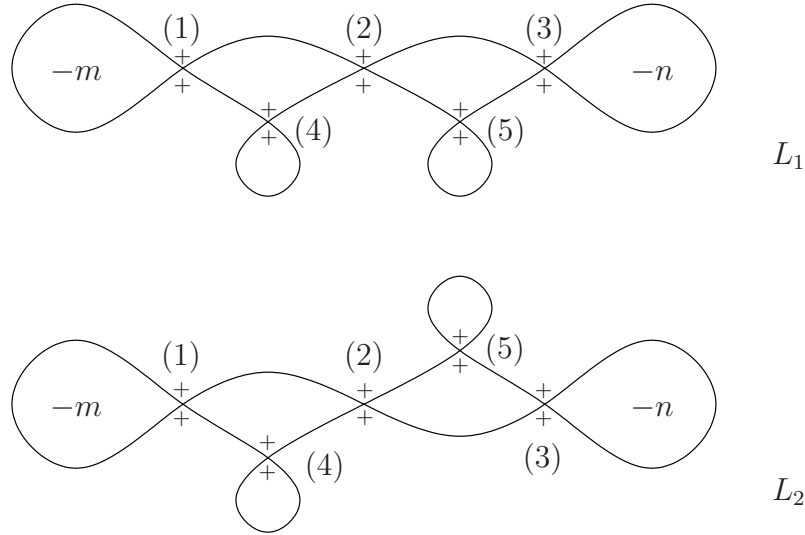


FIGURE 12. The knots L_1 and L_2 inside $L(p, 1)$ for $p \geq m+n+2$. The outer regions have defects of $m+n-p$ and the unlabeled inner regions all have defect equal to 0. The corners of the bounded regions of the diagram are labeled by $b+/a-$.

4. APPLICATIONS

4.1. An Example with Nontrivial Degree in the Fiber.

4.1.1. *The Knots L_1 and L_2 .* The two knots L_1 and L_2 in $L(p, 1)$ pictured in Figure 12 furnish the examples that prove the first part of Proposition 1.2. Assume that $p \geq n+m+2$ and that $n, m \geq 2$. A simple application of Proposition 2.6 shows that the diagrams in Figure 12 are indeed projections of Legendrian knots.

Proposition 4.1. *The Legendrian knots L_1 and L_2 are smoothly isotopic, but not Legendrian isotopic. If $n \neq m$, then L_1 represents a nontrivial class in $H_1(L(p, 1))$.*

By undoing the small loops at crossings 4 and 5, it is clear that L_1 and L_2 are topologically isotopic. After introducing some algebraic machinery in Section 4.1.2, the second part of the proposition will be proven in Section 4.1.3.

4.1.2. *The Characteristic Algebra.* Working directly with the DGAs $(\mathcal{A}_1, \partial_1)$ and $(\mathcal{A}_2, \partial_2)$ of the knots L_1 and L_2 is a difficult task. To facilitate computations for Legendrian knots in \mathbb{R}^3 , Ng introduced the **characteristic algebra** [22]. A direct adaptation of his definition to the circle bundle situation would still yield a complicated object. Since $F^0\mathcal{A}$ is an invariant sub-DGA of (\mathcal{A}, ∂) , however, it is possible to restrict the definition of the characteristic algebra to the lowest-energy generators.

Definition 4.2. Let I be the two-sided ideal in $F^0\mathcal{A}$ generated by the set

$$\{\partial x_i^0 \mid x_i^0 \text{ a generator in } F^0\mathcal{A}\}.$$

The low-energy **characteristic algebra** $\mathcal{C}^0(\mathcal{A}, \partial)$ of the filtered DGA (\mathcal{A}, ∂) is $(F^0\mathcal{A})/I$.

Suppose that $(\mathcal{A}_1, \partial_1)$ and $(\mathcal{A}_2, \partial_2)$ are related by an elementary isomorphism ϕ that sends x to $x' + v$. Since

$$(33) \quad \phi(\partial_1 x) = \partial_2 \phi(x) = \partial_2(x' + v),$$

the Leibniz rule shows that ϕ identifies I_1 and I_2 . Thus, say that $\mathcal{C}^0(\mathcal{A}_1, \partial_1)$ and $\mathcal{C}^0(\mathcal{A}_2, \partial_2)$ are **tame isomorphic** if \mathcal{A}_1 and \mathcal{A}_2 are tame isomorphic as algebras (after possibly adding “trivial” generators to both \mathcal{A}_i and I_i) so that the tame isomorphism identifies I_1 and I_2 .

Adding a stabilization \mathcal{E} to \mathcal{A} adds two generators e_1 and e_2 and the relation $e_2 = 0$ to $\mathcal{C}^0(\mathcal{A}, \partial)$. Thus, under stabilization, $\mathcal{C}^0(\mathcal{A}, \partial)$ changes by the addition of one generator and no further relations.

Put together, the equivalence relation of stable tame isomorphism on \mathcal{A} translates to:

Definition 4.3 (Ng [22]). Two characteristic algebras $\mathcal{C}^0(\mathcal{A}_1, \partial_1)$ and $\mathcal{C}^0(\mathcal{A}_2, \partial_2)$ are **equivalent** if they are tame isomorphic after adding a finite number of generators (with no additional relations) to each.

Theorem 3.11 and the discussion above prove:

Proposition 4.4 (Ng [22]). *If two Legendrian knots are Legendrian isotopic, then their low-energy characteristic algebras are equivalent.*

Remark. It is also possible to adapt Chekanov’s graded linearization method (see [5, 13, 18]) to this setting, but it cannot distinguish L_1 and L_2 . There are other situations in which it is useful, however.

4.1.3. *Proof of Proposition 4.1.* In order to calculate $\mathcal{C}^0(\mathcal{A}, \partial)$, it is necessary to know the differentials only of a_i^0 and b_i^0 ; the other generators of \mathcal{A} never come into play. With this in mind, drop the superscript 0 from the notation for the remainder of this section. The internal differential does not contribute, and the only disks that contribute to the external differential are those whose defect is 0 and do not contain a c^k term. In the case at hand, the only such disks come from the four regions in the center of the diagram. In particular, note that the regions at the ends have defect -1 for the b_1+ or b_3+ chords, so they do not contribute to $F^0\mathcal{A}$.

It follows that $\partial_i a_j = 0$ for $i = 1, 2$ and $j = 1, \dots, 5$. Further,

$$\begin{aligned} \partial_1 b_1 &= a_4 a_2 & \partial_2 b_1 &= a_4 a_2 \\ \partial_1 b_2 &= a_1 a_4 + a_5 a_3 & \partial_2 b_2 &= a_1 a_4 + a_3 a_5 \\ \partial_1 b_3 &= a_2 a_5 & \partial_2 b_3 &= a_5 a_2 \\ \partial_1 b_4 &= 1 + a_2 a_1 & \partial_2 b_4 &= 1 + a_2 a_1 \\ \partial_1 b_5 &= 1 + a_3 a_2 & \partial_2 b_5 &= 1 + a_2 a_3 \end{aligned}$$

Some simple manipulations of both characteristic algebras show that a_4 and a_5 are trivial in both $\mathcal{C}^0(\mathcal{A}_1, \partial_1)$ and $\mathcal{C}^0(\mathcal{A}_2, \partial_2)$. Further, $a_1 = a_3$ in $\mathcal{C}^0(\mathcal{A}_1, \partial_1)$. Thus, up to equivalence,

$$\begin{aligned} \mathcal{C}^0(\mathcal{A}_1, \partial_1) &= \mathbb{Z}_2\langle a_1, a_2 \rangle / (1 = a_1 a_2 = a_2 a_1), \\ \mathcal{C}^0(\mathcal{A}_2, \partial_2) &= \mathbb{Z}_2\langle a_1, a_2, a_3 \rangle / (1 = a_2 a_1 = a_2 a_3). \end{aligned}$$

These algebras cannot be equivalent, since all elements in $\mathcal{C}^0(\mathcal{A}_1, \partial_1)$ are invertible from both sides, while the element $a_2 \in \mathcal{C}^0(\mathcal{A}_2, \partial_2)$ is only invertible from the right. This finishes the proof of Proposition 4.1.

4.2. **An Example with Nontrivial Homology in the Base.** The second example presents two knots L_3 and L_4 whose projections to the base F represent nontrivial homology classes in $H_1(F)$, and hence provides the necessary examples to prove the second half of Proposition 1.2. Let γ be a simple closed curve that represents a nontrivial homology class in $H_1(F)$. Let α be an arbitrary contact form on E . Lift γ to a Legendrian curve $\tilde{\gamma}$ in E . Choose a closed form $\beta \in \Omega^1(F)$ whose

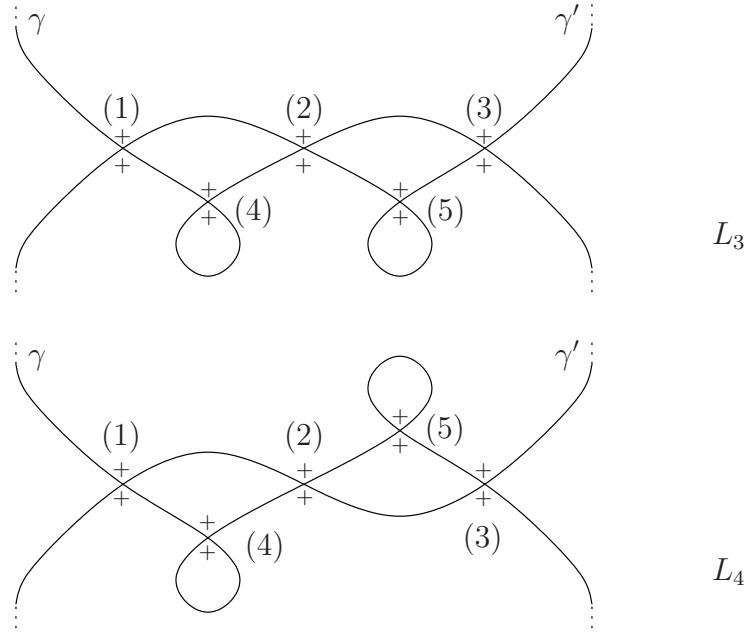


FIGURE 13. The knots L_3 and L_4 in $E \rightarrow F$. The region between γ and γ' and outside the the four central regions has defect 0, and the outer region has defect $p \leq -1$.

period around γ is equal to the negation of the holonomy of $\tilde{\gamma}$. For example, take β to be an appropriately scaled Poincaré dual to γ . As a result, γ is the projection of a closed Legendrian curve for the contact form $\alpha + \pi^*\beta$.

To form L_3 and L_4 , let γ' be a small translation of γ in F . Remove small segments of γ and γ' and glue in the middle portions of L_1 and L_2 . See Figure 13.

Proposition 4.5. *The Legendrian knots L_3 and L_4 are topologically isotopic, but not Legendrian isotopic.*

As with L_1 and L_2 , the only disks that contribute to the exterior differential on $F^0\mathcal{A}$ lie in the four central regions. Thus, the proof of Proposition 4.5 is the same as that of Proposition 4.1.

5. PROOF THAT \mathcal{A} IS A DGA

The goal of this chapter is to prove that $\partial \circ \partial = 0$, which will complete the proof of Theorem 3.11. In outline, the proof is similar to those in [5, 16], which, in turn, are combinatorial realizations of the standard proofs in Morse-Witten-Floer theory (see [2, 24], for example).

5.1. Outline of the Proof. It is convenient to prove the theorem on the level of power series. Suppose that \mathbf{x} is a generating power series in $\mathcal{A}_{(\Gamma^+, \vec{n})}$. Let $\mathbf{y}_1 \cdots \mathbf{y}_n$ represent a disk or flowline $f \in \Delta^U(x; y_1, \dots, y_n)$, and let $\mathbf{v}_1 \cdots \mathbf{v}_m$ represent a disk or flowline $g \in \Delta^U(y_i; v_1, \dots, v_m)$. Thus,

$$(34) \quad \mathbf{y}_1 \cdots \mathbf{y}_{i-1} \mathbf{v}_1 \cdots \mathbf{v}_m \mathbf{y}_{i+1} \cdots \mathbf{y}_n T^{-n(f)-n(g)}$$

is a term in $\partial(\partial\mathbf{x})$. The pair (f, g) is called a **broken disk at \mathbf{x}** . Two broken disks are equivalent if their component maps are.

The proof that $\partial(\partial\mathbf{x}) = 0$ proceeds by organizing the terms in $\partial(\partial\mathbf{x})$ — in other words, the broken disks at \mathbf{x} — into canceling pairs. The two maps that make up a broken disk can be

glued together at y_i to form a new immersed disk. The resulting **obtuse disk** satisfies all of the requirements of the definition of $\Delta^U(x; y_1, \dots, v_1, \dots, v_m, \dots, y_n)$ except that one corner covers three quadrants rather than one. Conversely, Section 5.4 shows that every obtuse disk splits into a broken disk in exactly two ways. Since the two broken disks comes from the same obtuse disk, they contribute identical terms to $\partial(\partial\mathbf{x})$. This will complete the proof.

5.2. An Equivalent Definition of ∂ . A more unified treatment of broken and obtuse disks may be achieved by altering the definition of the full differential. Instead of separating ∂ into internal and external pieces, all terms in the unified definition come from immersed disks in a modification of the diagram Γ . The motivation for this definition is the perturbation of the ‘‘Morse-Bott’’ contact form as described in [4].

The unified definition requires some combinatorial modifications to the diagram Γ . First, fix the following terminology. A **full lattice** is the set of lines $\{x = n\}_{n \in \mathbb{Z}} \cup \{y = n\}_{n \in \mathbb{Z}}$ in \mathbb{R}^2 . The intersections of these lines in the lattice are called **lattice points**. A **half-lattice** is the portion of a full lattice that lies below the diagonal line $y = x + \frac{1}{2}$. This line is called the **edge** of the half-lattice. There are two different concepts of distance on a half-lattice. Let (m, n) be a lattice point. The **distance δ to the edge** is given by either:

$$\begin{aligned} \delta_{ab}(m, n) &= m - n, \quad \text{or} \\ \delta_{cd}(m, n) &= m - n + 1. \end{aligned}$$

There is one last piece of terminology necessary: a **translation of a full lattice** is a linear map τ that sends lattice points to lattice points. A **translation of a half-lattice** is the restriction of a translation of a full lattice to the points in the half lattice whose images lie in the half-lattice.

The idea behind the modifications to Γ is to replace every special point by an embedding of a full or half lattice; see Figure 14. Fix a small neighborhood U of Γ . As pictured in Figure 15, replace a double point of Γ by a full lattice, split into half-lattices $\lambda(a)$ and $\lambda(b)$ that are matched up along their edges. Equip $\lambda(a)$ and $\lambda(b)$ with the distance function δ_{ab} . Label the quadrants around each double point in $\lambda(a)$ (resp., $\lambda(b)$) with $a+$ and $a-$ (resp., $b+$ and $b-$) as in Figure 15. Take note of the position of the adjacent c and d special points in Figure 15. The special points labeled c and d become embedded half-lattices $\lambda(c)$ and $\lambda(d)$, respectively, that are capped off along the lattice edge as pictured in Figure 16. Both are equipped with the distance function δ_{cd} . Let Γ_* denote $\Gamma \setminus \{\text{special points}\}$. Outside the lattices, U has the structure of the normal bundle $\nu\Gamma_*$.

Roughly speaking, the differential counts immersed disks whose boundaries lie in U and that have specified behavior in the lattices. More precisely, let $(D^2; z, w_1, \dots, w_m)$ be a disk with marked points ordered counter-clockwise on ∂D^2 , as in Section 3.2.1. Let x, y_1, \dots, y_m be special points of Γ . Define a smooth map $\rho : F \rightarrow F$ that retracts U onto Γ and collapses the half-lattices λ to their associated special points.

Definition 5.1. The **space of U -immersed marked disks** $\Delta^U(x; y_1, \dots, y_m)$ consists of immersions $f : D^2 \rightarrow F$ of marked disks that satisfy the following:

1. The map f sends z to a lattice point of $\lambda(x)$ and w_j to a lattice point of $\lambda(y_j)$.
2. For every marked point z (respectively, w_i), there exists a neighborhood N_z (resp., N_i) such that the map f sends $\partial D^2 \cap N_*$ to the lines of the corresponding half-lattice λ . Elsewhere, f sends ∂D either to a line of a half-lattice or to a section of $\nu\Gamma_*$. Further, $f|_{\partial D \setminus \{z, w_1, \dots, w_m\}}$ is smooth. Notice that $f(\partial D) \subset U$.
3. Let the neighborhoods N_* be as above. Near z and w_i , the image of $f|_{N_*}$ covers but one quadrant of Γ . At the lattice point $f(z)$, $f|_{N_z}$ covers one of the two quadrants labeled $x+$ and no other quadrants; say that f has a **positive corner** at x . At the lattice point $f(w_j)$,

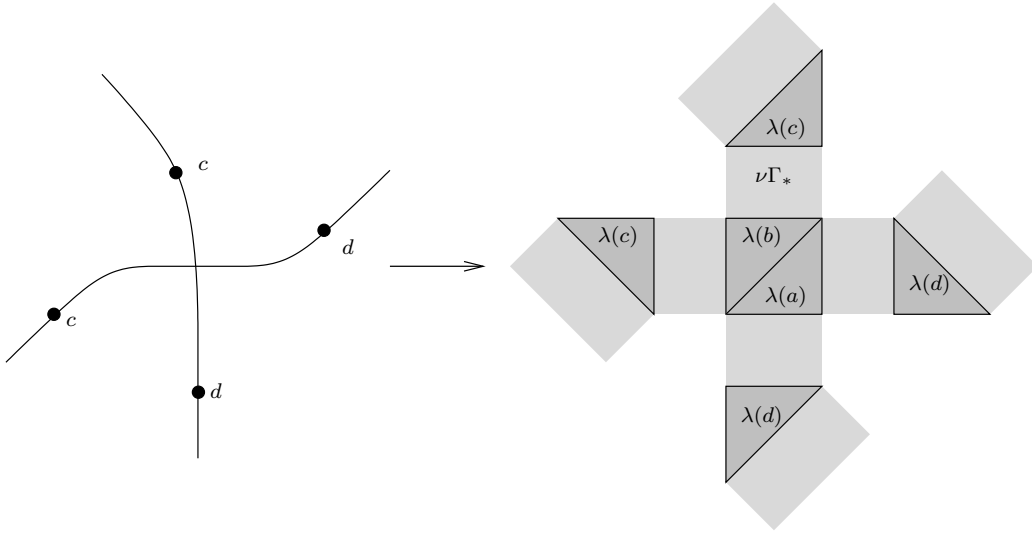
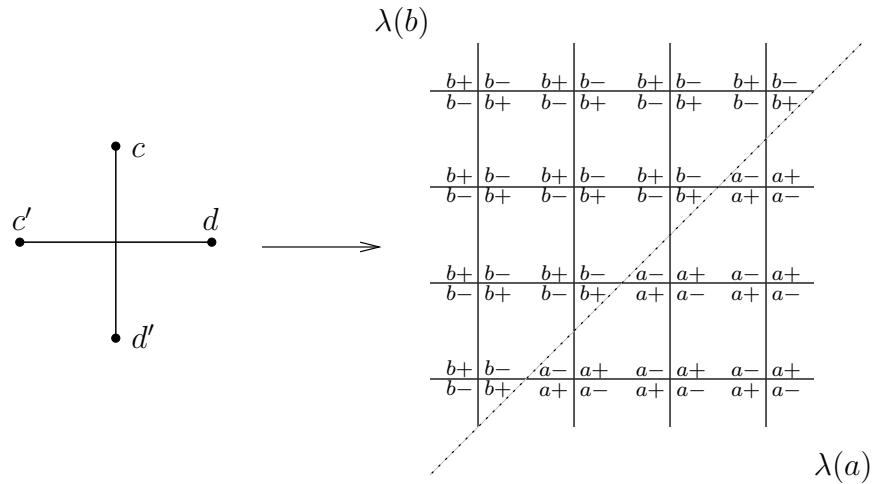


FIGURE 14. A schematic representation of the modified diagram.

FIGURE 15. A piece of the half-lattices $\lambda(a)$ and $\lambda(b)$ at a double point.

$f|_{N_j}$ covers one of the two quadrants labeled y_j- and no others; say that f has a **negative corner** at y_j .

4. The map satisfies:

$$\delta(f(z)) = \sum_j \delta(f(w_j)) - n(\rho \circ f; x, y_1, \dots, y_m).$$

Here, δ is either δ_{ab} or δ_{cd} , as appropriate. This is the **energy condition**.

Finally, say that two immersions f and g are **equivalent** in $\Delta^U(x; y_1, \dots, y_n)$ if there exists a smooth automorphism ϕ of the marked disk, neighborhoods N_z, N_1, \dots, N_m in D^2 ,¹⁰ and translations $\tau_x, \tau_{y_1}, \dots, \tau_{y_m}$ of the half-lattices $\lambda(x), \lambda(y_1), \dots, \lambda(y_m)$ (extended to translations of the full

¹⁰These neighborhoods may be different from those specified in the first condition.

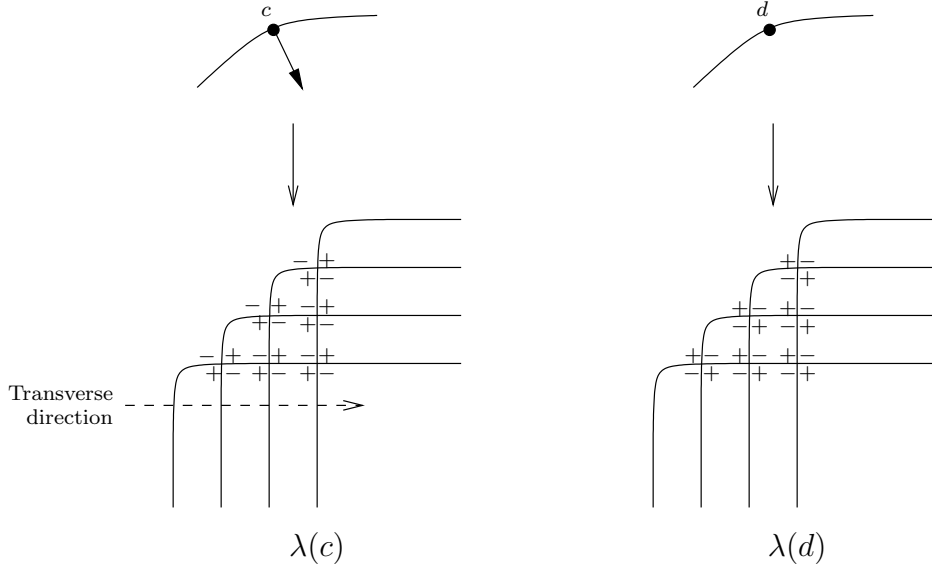


FIGURE 16. (a) A piece of the half-lattice $\lambda(c)$; (b) A piece of the half-lattice $\lambda(d)$.

lattice at the double points) so that:

$$(35) \quad \begin{aligned} f &= \tau_x \circ g \circ \phi && \text{in } N_z, \\ f &= \tau_{y_i} \circ g \circ \phi && \text{in } N_i, \\ \rho \circ f &= \rho \circ g \circ \phi. \end{aligned}$$

Remark. If $\text{Im } f \subset U$, then $\rho \circ f$ is no longer an immersion. Define the defect of such an f by summing the lengths of the chords that lie over double points:

$$(36) \quad 2\pi n(f; x, y_1, \dots, y_m) = \begin{cases} l(x) - \sum_{y_i \neq c_j} l(y_i) & x \neq d_j, \\ -\sum_{y_i \neq c_j} l(y_i) & x = d_j. \end{cases}$$

The defect of an “external” disk f with $\text{Im } f \not\subset U$ is defined to be the defect of $\rho \circ f$. Note that, by Lemma 2.3 and the proof of Proposition 5.2 below, the defect is always non-positive. Together with the energy condition, this implies:

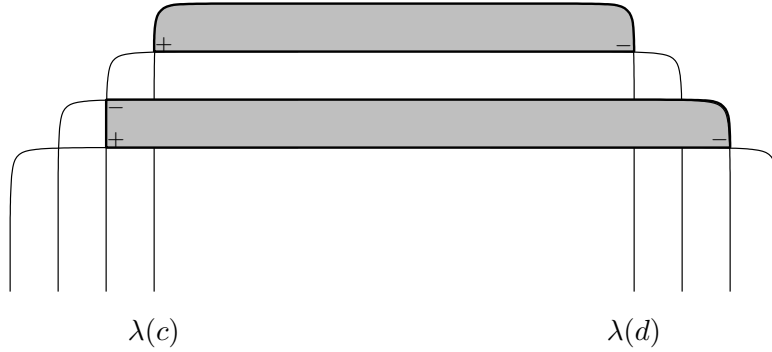
$$(37) \quad \delta(f(z)) \geq \sum_j \delta(f(w_j)).$$

Remark. Geometrically, a lattice point p in $\lambda(x)$ corresponds with the generator $x^{\delta(p)}$ in \mathcal{A} . The equivalence relation for Δ^U allows a single equivalence class to range over all possible combinations of corners in each lattice, while fixing the macroscopic geometry of the disk. Thinking of an equivalence class in Δ^U as a sum over all of these possibilities leads to a power series formula. This idea is realized by the following proposition:

Proposition 5.2. *The total differential ∂ defined in Section 3.2.3 is equivalent to:*

$$(38) \quad \partial \mathbf{x} = \sum_{f \in \Delta^U(x; y_1, \dots, y_m)} \mathbf{y}_1 \cdots \mathbf{y}_m T^{-n(f; x, y_1, \dots, y_m)}.$$

Proof. There are two types of maps in Δ^U : those whose image lies entirely inside U and the rest. As will be stated in Claims 5.3 and 5.4, the former type of map gives ∂_{int} , while the latter gives ∂_{ext} .

FIGURE 17. The corners of full flowlines in Δ^U .

Claim 5.3.

$$(39) \quad \partial_{int} \mathbf{x} = \sum_{\substack{f \in \Delta^U(x; y_1, \dots, y_m) \\ \text{Im } f \subset U}} \mathbf{y}_1 \cdots \mathbf{y}_m T^{-n(f; x, y_1, \dots, y_m)}.$$

Suppose that $f \in \Delta^U(x; y_1, \dots, y_m)$ satisfies $\text{Im } f \subset U$. Recall from Section 3.2.2 that the terms in the internal differential correspond to flowlines, half-flowlines, and vertex flowlines in Γ . The first step in proving the claim is to show that the image of $\rho \circ f$ (which is a line segment inside of Γ) coincides with one of these three types of flowlines. This follows from three facts:

1. The condition that $f|_{\partial D}$ is a section of $\nu\Gamma_*$ away from the special points shows that $\text{Im } f|_{\partial D}$ must run straight from one lattice to another without turning around mid-edge.
2. Since f is an immersion, Figure 16 shows that $\text{Im } f$ cannot pass through the lattices $\lambda(c)$ or $\lambda(d)$. In particular, if f has a corner at a c or a d , then $\text{Im}(\rho \circ f)$ must have an end there.
3. Since all of the corners of $\text{Im } f$ cover but one quadrant, $\text{Im}(\rho \circ f)$ can only have an end at or pass straight through a double point.

The next step is to show that “thickened flowlines” such as f give the terms in the definition of the internal differential. This requires a careful examination of the structure of the ends of each type of thickened flowline. Note that the description of the behavior of the ends of the flowlines in the lattices is unique up to the equivalence relation in Definition 5.1.

Suppose that $\text{Im}(\rho \circ f)$ coincides with a full flowline. Such a thickened flowline has either one or two corners in $\lambda(c)$. In either case, an examination of Figure 16(a) shows that at least one of the corners must be positive. Thus, by the third condition of the definition of Δ^U and Figure 16, a thickened flowline may only have a single negative corner in $\lambda(d)$. See Figure 17.

Regardless of the transverse direction, there are thick flowlines with a single positive corner that leave the diagram of $\lambda(c)$ in Figure 16 both down and to the right. The latter is shown at the top of in Figure 17. In the notation of Figure 9, these give the $\mathbf{d}'_1 + \mathbf{d}'_2$ terms in $\partial_{int} \mathbf{c}$.

If f is a thick flowline that has two corners in $\lambda(c)$ and leaves the lattice to the right, then it has the form depicted at the bottom of Figure 17. In counter-clockwise order, the flowline has a positive corner in $\lambda(c)$, a negative corner in $\lambda(d)$, and finally a negative corner back in $\lambda(c)$. This gives the word $\mathbf{d}'_2 \mathbf{c}$ in $\partial_{int} \mathbf{c}$. The order of the \mathbf{c} and \mathbf{d} is reversed for flowlines that leave downward, which gives the $\mathbf{c} \mathbf{d}'_1$ term in $\partial_{int} \mathbf{c}$. Overall, the full flowlines contribute $(1 + \mathbf{c}) \mathbf{d}'_1 + \mathbf{d}'_2 (1 + \mathbf{c})$ to $\partial_{int} \mathbf{c}$.

The analysis of the other types of flowlines in Figure 17 is similar. Adding up the contributions yields ∂_{int} and hence proves Claim 5.3.

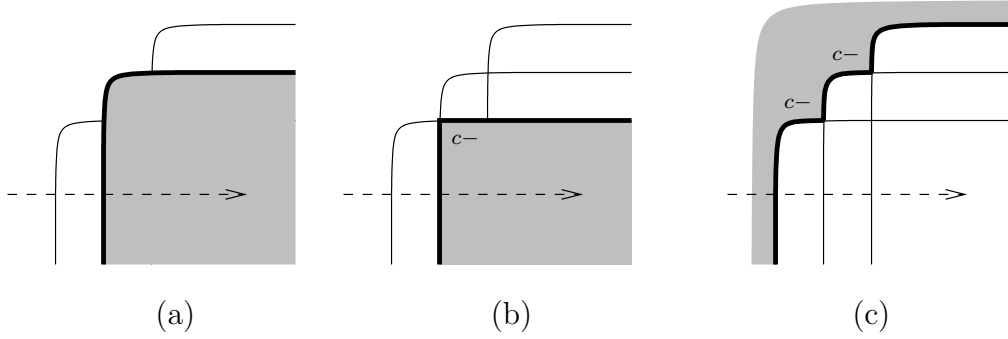


FIGURE 18. Corners of f in $\lambda(c)$ when the transverse direction points into f and f (a) has no corners at a c or (b) has a corner at a c ; (c) the corners when the transverse direction points out of f .

Claim 5.4.

$$(40) \quad \partial_{ext} \mathbf{x} = \sum_{\substack{f \in \Delta^U(x; y_1, \dots, y_m) \\ \text{Im } f \not\subset U}} \mathbf{y}_1 \cdots \mathbf{y}_m T^{-n(f; x, y_1, \dots, y_m)}.$$

Let $g \in \Delta(x; y'_1, \dots, y'_n)$. It suffices to show that the terms in $\partial_{ext} \mathbf{x}$ that come from g are the same as those in

$$(41) \quad \sum_{\substack{f \in \Delta^U(x; y_1, \dots, y_m) \\ \rho \circ f = g}} \mathbf{y}_1 \cdots \mathbf{y}_m T^{-n(f; x, y_1, \dots, y_m)}.$$

Let f be a map that contributes to the sum in (41). The maps $\rho \circ f$ and g share their positive corner and their negative corners at double points. Further, up to equivalence, g uniquely determines $\text{Im } f$ in $\lambda(x)$ and in the double point lattices. The structure of the half lattices $\lambda(c)$ and $\lambda(d)$ shows that $\rho \circ f$ can send neither a positive marked point to a c , nor a negative marked point to a d . The proof of the claim now rests on the reconciliation of the marked points that f and g send to c points.

The fourth and final condition in the definition of $\Delta(x; y'_1, \dots, y'_n)$ states that if $g|_{\partial D^2}$ crosses a special point labeled c , then that c must be the image of a marked point. That requirement lead to a $(1 + \mathbf{c})$ or a $(1 + \mathbf{c})^{-1}$ (depending on the transverse direction at c) in the word generated by g . If the transverse direction at c points into $\text{Im } g$, then, as shown in Figures 18(a) and (b), the map f may either pass through $\lambda(c)$ without a marked point or may have a single negative c corner. The former map gives the 1, while the latter gives the \mathbf{c} in $(1 + \mathbf{c})$. On the other hand, if the transverse direction points out of $\text{Im } g$, then, as shown in Figure 18(c), the map f may have any number of negative corners in $\lambda(c)$. Up to equivalence, f is determined by the number of c corners in each lattice $\lambda(c)$. Since

$$(1 + \mathbf{c})^{-1} = 1 + \mathbf{c} + \mathbf{c}\mathbf{c} + \mathbf{c}\mathbf{c}\mathbf{c} + \cdots,$$

summing the contributions of all possible maps f gives the same terms as does g in the original definition. This completes the proof of Claim 5.4, and hence the proof of Proposition 5.2. \square

5.3. Gluing Broken Disks. In light of the unified definition of the differential, the definition of a broken disk needs to be modified. Suppose that $f \in \Delta^U(x; y_1, \dots, y_n)$ and $g \in \Delta^U(y_i; v_1, \dots, v_m)$. Denote the marked points in the domain of f by $\{z, w_1, \dots, w_n\}$ and those in the domain of g by $\{z', w'_1, \dots, w'_m\}$. The pair (f, g) is a **broken disk at \mathbf{x}** if $f(w_i) = g(z')$. Up to the equivalence

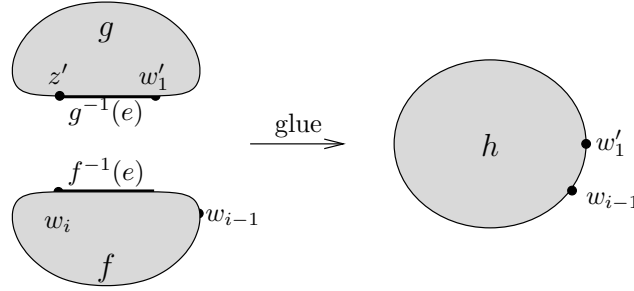


FIGURE 19. Gluing the domains of f and g along $f^{-1}(e)$ and $g^{-1}(e)$.

relation in Δ^U , certain extra assumptions may be made about the form of f and of g . Since the corners of f and g match at y_i , the images of f and g share an edge e in the lattice $\lambda(y_i)$. Assume that they share this edge until either f or g has another corner. The edge e has one end in $\lambda(y_i)$ and another in either $\lambda(y_{i-1})$ or $\lambda(v_1)$, whichever comes first.¹¹ The notion of which corner comes first is unambiguous if $v_1 \neq y_{i-1}$. If, on the other hand, $v_1 = y_{i-1}$, then the geometry of the lattices and the energy condition dictate the order of the corners.

For notational convenience, suppose that the ends of e lie in $\lambda(y_i)$ and $\lambda(v_1)$. Glue the domains of f and g along $f^{-1}(e)$ and $g^{-1}(e)$ as shown in Figure 19. Remove the marked points w_i and z' , but retain w'_1 . Define a new map $h : D^2 \rightarrow F$ by piecing together f and g on the glued domain and smoothing as necessary. By the discussion above, h covers three quadrants at $h(w'_1)$; this is the **obtuse corner** for h . Say that the obtuse corner is **positive** if two of the three quadrants covered are positive, and **negative** otherwise. The result is an **obtuse disk**, which satisfies all of the requirements of Definition 5.1 for $\Delta^U(x; y_1, \dots, v_1, \dots, v_m, \dots, y_n)$, except for the existence of one obtuse corner. The map h satisfies the energy condition because:

$$\begin{aligned}
 \delta(h(z)) &= \delta(f(z)) \\
 &= \sum_j \delta(f(w_j)) - n(f) \\
 (42) \quad &= \sum_{j \neq i} \delta(f(w_j)) + \sum_k \delta(g(w'_k)) - n(f) - n(g) \\
 &= \sum_j \delta(h(w_j)) - n(h).
 \end{aligned}$$

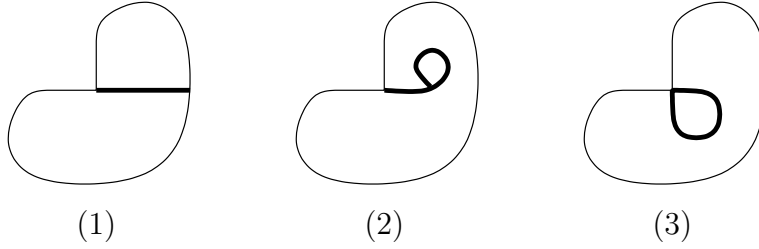
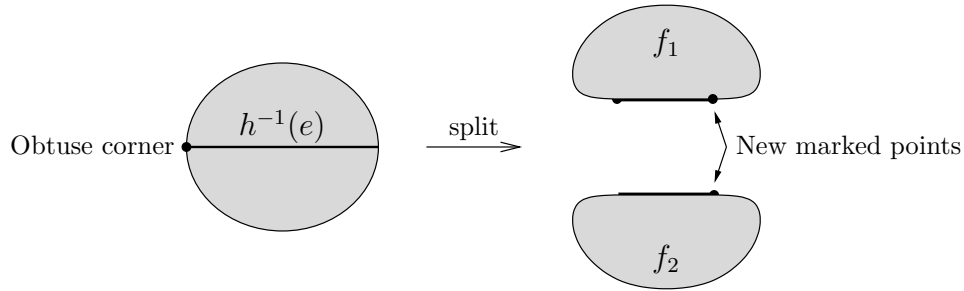
The last line requires that the defects combine correctly:

$$(43) \quad n(f; x, y_1, \dots, y_n) + n(g; y_i, v_1, \dots, v_m) = n(h; x, y_1, \dots, v_1, \dots, v_m, \dots, y_n).$$

This follows directly from the definition of the defect (and equation (36) if any of f , g , or h are flowlines). Thus, the $-n(h; \dots)$ is the exponent of T in equation (34), regardless of which broken disk was glued to form it.

5.4. Degeneration of Obtuse Disks. It remains to show that any obtuse disk h splits into exactly two different broken disks. Suppose that h has a positive corner at x and negative corners at y_1, \dots, y_n . Suppose further that the obtuse corner lies in $\lambda(o)$, which may be either $\lambda(x)$ or

¹¹If $i = 1$, then y_0 is taken to be x . Similarly, if $m = 0$, then v_1 is taken to be y_i . Clearly, it suffices to treat the case $n \geq 1$.


 FIGURE 20. The three ending conditions for the edge e (shown in bold).

 FIGURE 21. Splitting the domains along $h^{-1}(e)$.

some $\lambda(y_i)$. There are two line segments in $\lambda(o)$ that start at the obtuse corner and point into the interior of $\text{Im } h$. Each segment e splits h into a broken disk as follows: extend e along the lattice and, if necessary, by sections of $\nu\Gamma_*$ and along subsequent lattices until one of the following occurs:

1. The segment intersects the smooth part of the boundary of the obtuse disk,
2. The segment intersects itself, or
3. The segment returns to the obtuse corner.

See Figure 20. Notice that all three ending conditions must occur within some lattice $\lambda(p)$, though there is some ambiguity about the strand upon which e enters $\lambda(p)$. The preimage $h^{-1}(e)$ divides the domain D^2 into two sub-disks D_1^2 and D_2^2 . Parameterize e by $[0, 1]$ so that $e(0) \in \lambda(o)$ and $e(1) \in \lambda(p)$. Place an extra marked point at $h^{-1}(e(1))$ in each of the new domains, as shown in Figure 21. Let $f_j = h|_{D_j^2}$ for $j = 1, 2$. One of the f_i has a positive corner at $e(1)$; the other a negative corner at $e(1)$.¹² Since there are exactly two possible splitting segments e , the following lemma completes the proof of Theorem 3.11:

Lemma 5.5. *There exists a unique choice for the behavior of e and h (up to equivalence) in $\lambda(o)$ so that the pair (f, g) is a broken disk.*

Proof. Since $f(h^{-1}(e(1))) = g(h^{-1}(e(1)))$, it is sufficient to show that f and g are in the appropriate Δ^U space. Consider each of the conditions in Definition 5.1 in turn.

5.4.1. *Conditions 1 and 2.* Both f and g are immersions since h is. They inherit the first two properties of Definition 5.1 from h and the construction of e in $\lambda(o)$ and $\lambda(p)$.

5.4.2. *Condition 3.* The third property in Definition 5.1 requires the existence of a unique (up to equivalence) choice of e and h so that each f_j has exactly one positive corner. After the splitting construction, there are two positive corners to distribute between the f_j : one from h and the other

¹²It is possible that the second disk has two negative corners in case (3).

at $e(1)$. Thus, for the third condition, the lemma reduces to showing that there exists a unique choice of behavior for e and h in $\lambda(o)$ such that the positive corner at $e(1)$ does not lie in the same disk as does the positive corner from h . There are three cases:

Neither $\text{Im } f$ nor $\text{Im } g$ lies in U : In this case, $\lambda(p)$ must be a double-point lattice. Since the splitting edge e must leave the lattice $\lambda(o)$, there is complete freedom of choice about where e enters $\lambda(p)$. In particular, e may end at either an a corner or a b corner, and only one of these choices will place the positive corner at $e(1)$ in the correct disk.

Both $\text{Im } f$ and $\text{Im } g$ lie in U : If $\text{Im } f_j \subset U$, then the argument at the beginning of the proof of Proposition 5.2 shows that the image of $\rho \circ f_j$ coincides with that of a flowline. It is possible, however, for f_j to have more or less than one positive corner. For convenience, call such maps f_j “flowlines” for the rest of the section, even though they might not contribute to ∂_{int} .

With this in mind, the second case follows from:

Claim 5.6. *No flowline can have all negative corners.*

Proof. An inspection of the lattices in Figures 15 and 16 shows that no vertex flowline can have all negative corners, and that every flowline that has an end in $\lambda(c)$ has at least one positive corner. This leaves the case of a half-flowline from a double point to a d , but any such half-flowline must have at least one positive corner in either $\lambda(a)$ or $\lambda(b)$. \square

Only one of $\text{Im } f$ or $\text{Im } g$ lies in U : In other words, one of the f or g is a flowline (say that f is) and the other is an external disk. Claim 5.6 shows that f has at least one positive corner. The goal is to show that f has *exactly* one positive corner. Suppose, instead, that f has two positive corners for *any* choice of the behavior of e and h in $\lambda(p)$, and proceed by contradiction.

First, suppose that f is a vertex flowline in some $\lambda(d)$. If this were the case, then $e(1)$ would also be in $\lambda(d)$, so g would have a corner in $\lambda(d)$. This corner must be positive, which contradicts the assumption that the flowline contains both positive corners. Thus, f cannot be a vertex flowline in $\lambda(d)$.

Next, suppose that f is a full flowline. As before, g cannot have any corners in $\lambda(d)$, so any corner of f in $\lambda(d)$ is also a corner of h . The energy condition and a quick examination of Figure 16 show that while f must have a negative corner in $\lambda(d)$, it cannot have a positive corner there. Thus, the flowline can only have a single negative corner in $\lambda(d)$. This gives a contradiction, for a full flowline can have at most one positive corner in $\lambda(c)$.

If f is a half-flowline to a d , the arguments above show that f must have two positive corners in $\lambda(a) \cup \lambda(b)$. Since the obtuse disk has but one positive corner, one of the positive corners of the flowline must be at $e(1)$. As shown in Figure 22, either shifting e or shifting the entire obtuse disk h in $\lambda(a) \cup \lambda(b)$ gives a flowline with only one positive corner, which is a contradiction.

Next, consider a half-flowline from a c . In order to have two positive corners, the flowline must have corners that cover either both an $a-$ and an $a+$ or both a $b+$ and a $b-$ in the double point lattice. If both of the corners in the double point lattice are corners of the obtuse disk, then an inspection of Figure 15 shows that the obtuse disk would not satisfy (37). If $e(1)$ lies at the negative corner of the flowline in the double point lattice, then the external disk would have a positive corner, which is a contradiction. Finally, if the flowline and the external disk are glued together at the flowline’s positive corner, then the edge e may be shifted so that the external disk has a positive corner; see Figure 23. In sum, the existence of any half-flowline from a c with two positive corners leads to a contradiction.

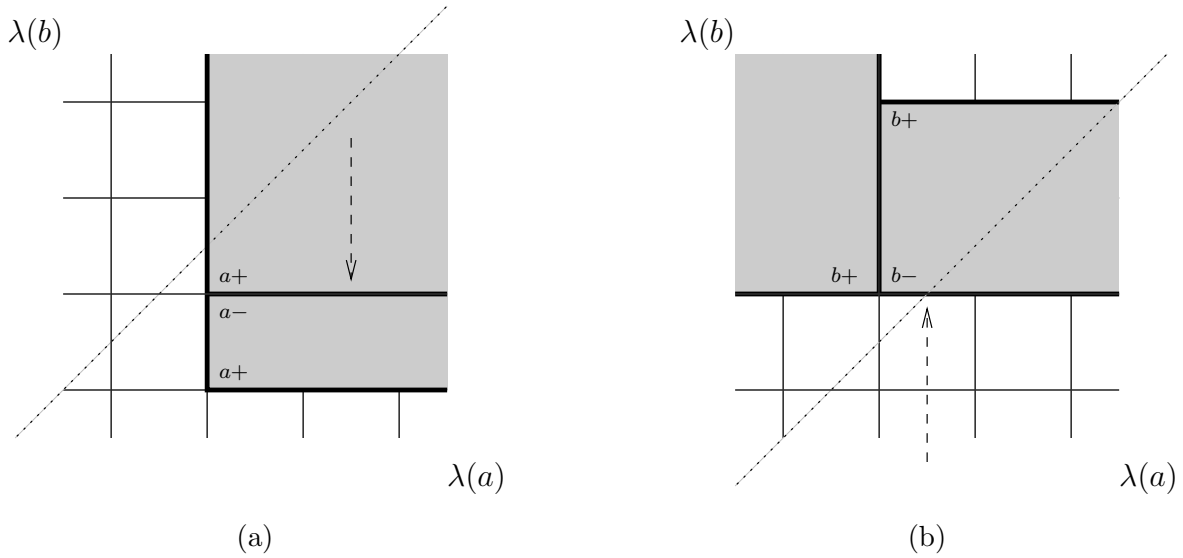


FIGURE 22. (a) Shifting e down until it meets the boundary of h at an a crossing yields a flowline with only one positive corner; (b) shifting the boundary of the obtuse disk up until e meets the boundary at a b corner yields a flowline with only one positive corner. The other cases differ by a reflection.

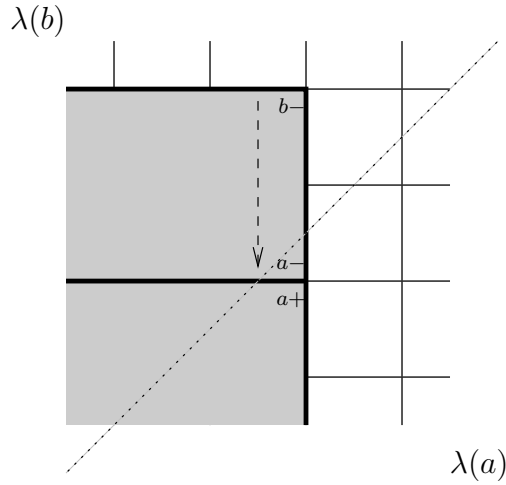
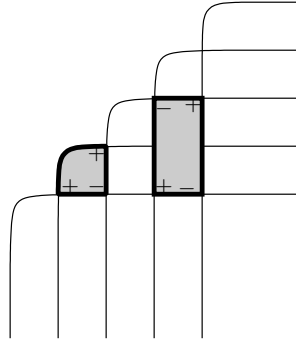
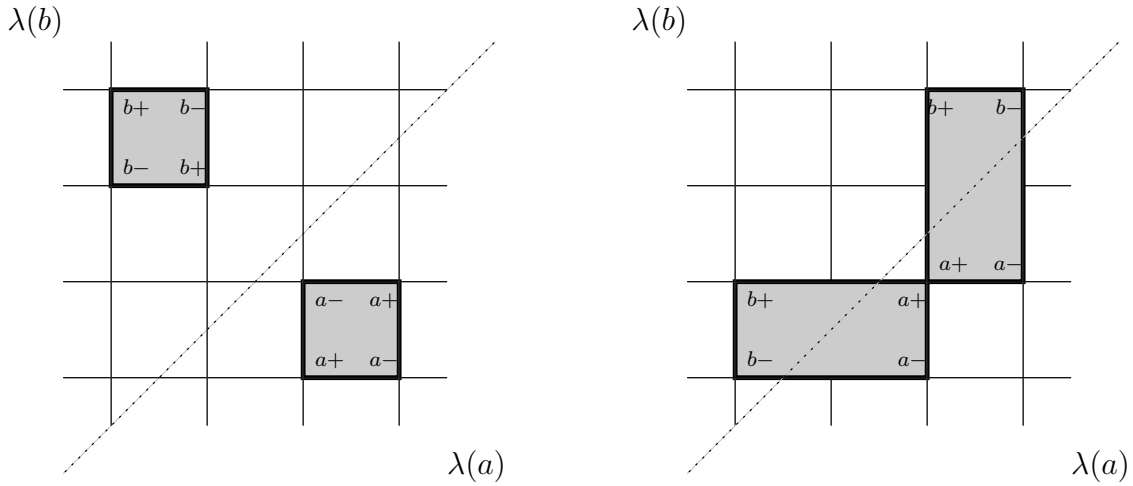


FIGURE 23. The segment e may be shifted down so that the external disk has a positive corner in $\lambda(a) \cup \lambda(b)$.

Suppose that the flowline is a vertex flowline in $\lambda(c)$; the possibilities are pictured in Figure 24. The vertex flowline must have a positive corner at $e(1)$; otherwise, g would have a positive corner. Once the gluing is performed, however, there is always a negative corner that is further away from the lattice edge than the remaining positive corner. But this is impossible by (37), giving the desired contradiction.

Finally, Figure 25 depicts the possible vertex flowlines in $\lambda(a) \cup \lambda(b)$. All of these satisfy:

Claim 5.7. *The sum of the distances of the to the lattice edge, counted with sign, is zero.*

FIGURE 24. Vertex flowlines in $\lambda(c)$.FIGURE 25. Vertex flowlines in $\lambda(a) \cup \lambda(b)$.

Proof. Put coordinates on the full lattice $\lambda(a) \cup \lambda(b)$ by placing the origin at one of the nodes of $\lambda(b)$ that lies closest to the lattice edge. Then the distance δ_{ab} to the lattice edge is given by:

$$(44) \quad \delta_{ab}(m, n) = \begin{cases} m - n - 1 & (m, n) \in \lambda(a) \\ n - m & (m, n) \in \lambda(b). \end{cases}$$

In every vertex flowline in Figure 25, the corners in $\lambda(a)$ can be paired as $a + / a -$ (if they exist). Thus, the -1 terms that appear in (44) cancel from $\sum_{\text{corners}} \delta_{ab}(i, j)$. Every coordinate appears in the sum twice with opposite sign since consecutive corners are either labeled with the same letter that have opposite signs or are labeled with opposite letters that have the same sign. The claim follows. \square

As in the argument for the vertex flowlines in $\lambda(c)$, the flowline must have a positive corner at $e(1)$. The claim above shows that the sum of the distances from the negative corners to the lattice edge is greater than that of the remaining positive corner. This contradicts (37), and finishes the proof that f and g satisfy the third condition of Definition 5.1.

5.4.3. *The Energy Condition.* The last thing to show is that f and g satisfy the energy condition. By (42) and the assumption that h satisfies the energy condition, if one of the two satisfy the energy condition, then the other will as well. The goal, then, is to show that the behavior of e and h can be chosen so that either f or g satisfies the energy condition.

First, suppose that both f and g are external disks, and that f contains the positive corner from h . There is sufficient freedom to shift e in $\lambda(p)$ so that $\delta(g(z')) = \delta(e(1)) = \sum_j \delta(g(w_j)) - n(g)$. Thus, after the shift, g satisfies the energy condition.

From now on, assume that at least one of f or g is a flowline. As in Claim 5.7, the sum of the distances of the corners of a true flowline can be easily read off from its combinatorics. If the sum of the distances, counted with sign, is equal to the negation of the defect, then the flowline satisfies the energy condition. The following claim results from direct computations using the usual coordinates on full and half lattices:

Claim 5.8. *Suppose f is a flowline that satisfies the first three conditions of Definition 5.1.*

1. *If f is a vertex flowline, then f satisfies the energy condition.*
2. *If f is a full flowline or a half-flowline to a d , then the contribution to the sum of the distances by the corners in an end in $\lambda(x)$ is equal to the width of the flowline in $\lambda(x)$. The width contributes positively at the end with the positive corner, and negatively in $\lambda(d)$.*
3. *If f is a half-flowline from a c , then the contribution to the sum of the distances in $\lambda(c)$ is the width of the flowline and the contribution at the double point is the negation of the width of the flowline minus one.*

The claim shows that the energy condition holds if the flowline is a vertex flowline. Further, if e and h can be arranged so that the widths at the ends of the flowline match up, then the flowline would satisfy the energy condition, and Lemma 5.5 would follow. Note that the extra -1 at the double-point end of the half-flowline from a c corresponds with the defect of the half-flowline. Thus, it remains to prove that e and h may be chosen so that the widths of the ends of the flowlines match up.

There are two broad cases to consider.

The segment e runs along the length of the flowline f : First, suppose that $e(1)$ lies in $\lambda(c)$ or $\lambda(d)$. If the other component of the purported broken disk is an external disk, then e may be shifted to realize any width for the flowline. For an example of this, see Figure 26. In particular, e can be shifted until the width of f in $\lambda(c)$ or $\lambda(d)$ matches the width at the other end of f (which is determined by the choice of h).

So just consider the case where both f and g are flowlines. If $e(1)$ lies in $\lambda(d)$, then, since either f or g must have a positive corner there, one component is a vertex flowline and hence already satisfies the energy condition. Otherwise, if $e(1)$ lies in $\lambda(c)$, then h must have a positive corner in $\lambda(c)$. The energy condition on h implies that the width of h in $\lambda(c)$ bounds the width of h in any other lattice. In particular, the width of h bounds the width of f , so e may be chosen in $\lambda(c)$ so as to realize the appropriate width.

Finally, if $e(1)$ lies in a double-point lattice, similar arguments show that, again, either e may be shifted to realize any width or that the widths in other lattices are bounded by the width in the double-point lattice.

The segment e forms the end of the flowline: The arguments are entirely similar in this case. Instead of shifting the segment e in the lattice containing $e(1)$, it is necessary to shift the side of h in which $e(1)$ lies. For example, see Figure 22(b). As before, either the positive corner of h lies in the flowline and gives a necessary bound on the width of the flowline elsewhere, or the side of h in which $e(1)$ lies has complete freedom to shift to the required width.

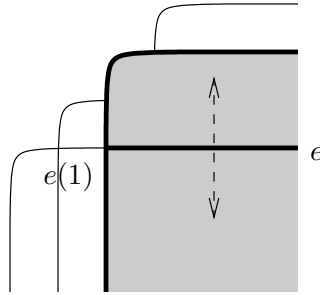


FIGURE 26. If $e(1) \in \lambda(d)$, the obtuse disk has no corner in $\lambda(d)$, and the other disk is external, then the segment can be shifted to realize any width for the flowline.

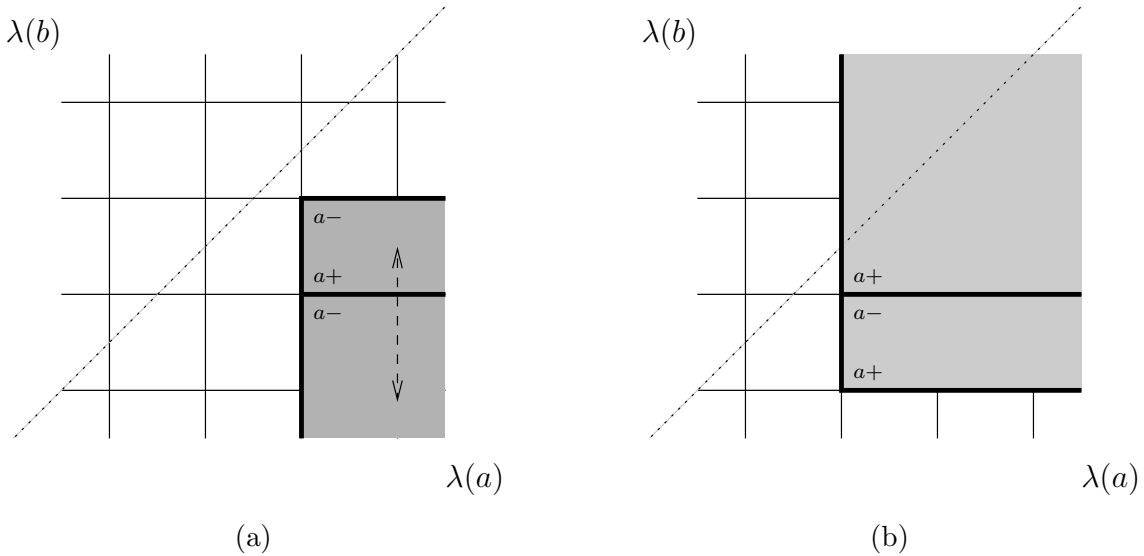


FIGURE 27. If $e(1) \in \lambda(a) \cup \lambda(b)$ and the flowline is a half-flowline to a d , then either (a) e may be shifted to realize any width, or (b) the width at d is bounded by $\delta(a+)$ so any e as shown works.

This finishes the proof of Lemma 5.5, and hence completes the proof of Theorem 3.11. □

6. PROOF OF INVARIANCE

The final loose end is the proof of Theorem 3.15, i.e. that the stable tame isomorphism type of (\mathcal{A}, ∂) is an invariant of Legendrian knots. The proof consists of somewhat technical combinatorial arguments generalizing those in [5, 16] to the contact circle bundle setting.

6.1. Choices at c and d Points.

6.1.1. *Transverse Directions at c .* The first part of Theorem 3.15 states that the stable tame isomorphism type of the DGA of a knot diagram is independent of the choices of transverse directions at the edge points labeled with c_i . Let c label one of these points, and let (\mathcal{A}, ∂) and $(\mathcal{A}', \partial')$ be the DGAs given by the two choices of a transverse direction. Define a homomorphism $\phi : \mathcal{A} \rightarrow \mathcal{A}'$ to be the identity on all generators besides c^k , $k = 1, 2, \dots$, and to map the generators c^k according

to the power series formula

$$(45) \quad \phi(1 + \mathbf{c}) = (1 + \mathbf{c}')^{-1}.$$

Since the generating power series \mathbf{c} contains no constant term, this indeed gives a tame isomorphism. The first part of Theorem 3.15 follows from:

Lemma 6.1. *ϕ is a chain map.*

Proof. First, let $\mathbf{x} \neq \mathbf{c}$ be a generating power series of \mathcal{A} . The term $(1 + \mathbf{c})^{\pm 1}$ appears in $\partial \mathbf{x}$ if and only if $(1 + \mathbf{c}')^{\mp 1}$ appears in $\partial' \mathbf{x}$, so ϕ is a chain map on \mathbf{x} . That ϕ is a chain map on \mathbf{c} is the result of a direct computation using Definition 3.10. \square

6.1.2. *Choice of c_1 .* The second part of Theorem 3.15 asserts that the stable tame isomorphism type of the DGA of a knot diagram does not depend on whether a given edge point has a c_i or d_i label. To prove this, it suffices to show that the tame isomorphism type of the DGA remains unchanged when the c and d labels are cyclically shifted; i.e. the point labeled with d_i becomes c_i and the point labeled c_i becomes d_{i-1} .

The idea is to define a homomorphism $\phi : (\mathcal{A}, \partial) \rightarrow (\mathcal{A}', \partial')$ via local contributions at each double point. First, some notation is necessary. Let \mathbf{y}_i be the contribution to $\partial_{int} \mathbf{c}$ of the half-flowline from c_i to the double point between c_i and d_i . Similarly, let \mathbf{x}_i come from the half-flowline from c_i to the double point between c_i and d_{i-1} . Suppose that the special points near a double point are labeled as in Figure 28.

- If d passes through the double point,¹³ then:

$$(46) \quad \phi(\mathbf{d}) = \mathbf{d} + \mathbf{y}.$$

Note that the T is included in \mathbf{y} .

- If d' passes through the double point, then:

$$(47) \quad \phi(\mathbf{d}) = \mathbf{d} + \mathbf{y}'.$$

- If c passes through the double point, then:

$$(48) \quad \begin{aligned} \phi(\mathbf{a}) &= \mathbf{a}(1 + \mathbf{c})^{-1}, \\ \phi(\mathbf{b}) &= (1 + \mathbf{c})\mathbf{b}. \end{aligned}$$

- If c' passes through the double point, then:

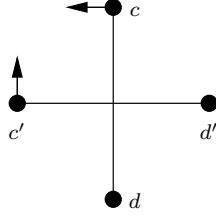
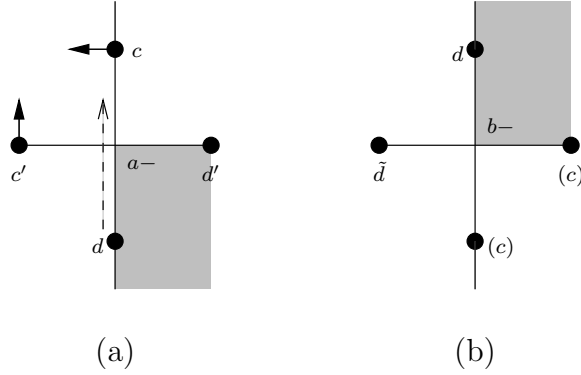
$$(49) \quad \begin{aligned} \phi(\mathbf{a}) &= (1 + \mathbf{c}')^{-1}\mathbf{a}, \\ \phi(\mathbf{b}) &= \mathbf{b}(1 + \mathbf{c}'). \end{aligned}$$

Only two of these possibilities can occur at any given double point. Using the results of Section 6.1.1, it is easy to see that if the transverse direction at a c changes in Figure 28, then $(1 + \mathbf{c})^{\pm 1}$ changes to $(1 + \mathbf{c})^{\mp 1}$ in (48) and (49).

The full map ϕ comes from taking the local contributions first from the d moves and then the c moves into account, one at a time. By Lemma 3.13, each of these steps is a tame isomorphism of algebras. It follows that ϕ is the composition of finitely many tame isomorphisms, and hence is itself a tame isomorphism of algebras.

It remains to show that ϕ is a chain map. The proof may be separated into two steps.

¹³In other words, if d gets shifted to the position previously occupied by c .

FIGURE 28. Labels of special points around a double point in the definition of ϕ .FIGURE 29. (a) Disks in $\partial_{ext}\mathbf{d}$; (b) Disks in $\partial'_{ext}\mathbf{d}$. The points labeled (c) are some unspecified c_i -labeled edge points.

$\phi\partial_{ext} = \partial'_{ext}\phi$: First, suppose that a special point w lies outside Figure 28. Further, suppose that a disk in $\partial_{ext}\mathbf{w}$ has a negative corner at the double point in Figure 28. If d of d' pass through the double point, then, locally, nothing changes in $\partial_{ext}\mathbf{w}$. If c passes through the double point and the boundary of the disk passes through c before the shift, then:

1. The position of the $(1 + \mathbf{c})^{\pm 1}$ factor with respect to the corner at the double point is the same in $\partial_{ext}\mathbf{w}$ and in the image of the double point corner under ϕ .
2. If $(1 + \mathbf{c})^{\pm 1}$ appears in $\partial_{ext}\mathbf{w}$, then ϕ contributes $(1 + \mathbf{c})^{\mp 1}$.

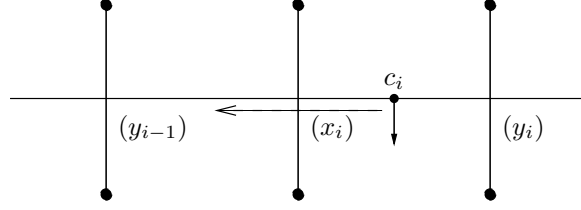
Thus, the $(1 + \mathbf{c})^{\pm 1}$ factors cancel in $\phi\partial_{ext}\mathbf{w}$. On the other hand, after the shift of the c , the disk no longer passes through c , so there are no $(1 + \mathbf{c})^{\pm 1}$ factors in $\partial'_{ext}\phi\mathbf{w}$. Hence, the local contributions of $\partial'_{ext}\phi\mathbf{w}$ and $\phi\partial_{ext}\mathbf{w}$ agree.

If the boundary of the disk passes through c after the shift, then the position and the exponent of $(1 + \mathbf{c})^{\pm 1}$ are both the same for the external disk after the shift and for the image of the double point corner under ϕ . Thus, once again, the local contributions of $\partial'_{ext}\phi\mathbf{w}$ and $\phi\partial_{ext}\mathbf{w}$ agree. Since the argument for c' is exactly the same, this finishes the case when w lies outside of Figure 28 and $\partial_{ext}\mathbf{w}$ has a negative corner at the double point.

Next, consider the special point d in Figure 28. Suppose that d passes through the double point and that a disk in $\partial_{ext}\mathbf{d}$ has a negative corner at the double point as in Figure 29. Such disks represent words of the form \mathbf{Va} . The terms in $\phi(\mathbf{Va})$ differ from \mathbf{Va} at negative corners through which a c passes. This is exactly the situation considered above. Thus, by abusing notation, write $\phi(\mathbf{Va}) = \mathbf{Va}$.

On the other hand, $\mathbf{y} = \mathbf{ba}T$ and so $\phi(\mathbf{d}) = \mathbf{d} + \mathbf{ba}T$. The differential $\partial'_{ext}(\mathbf{d} + \mathbf{ba}T)$ yields three types of disks on the right side of Figure 29(b):

1. $\partial'_{ext}\mathbf{d}$ gives the disks pictured in Figure 29(b).
2. $\mathbf{b}\partial'_{ext}(\mathbf{a})T$ matches the disks in $\partial'_{ext}\mathbf{d}$.

FIGURE 30. The local configuration for c shifting to the left.

3. $\partial'_{ext}(\mathbf{b})\mathbf{a}T$ matches $\mathbf{V}\mathbf{a}$ and hence matches $\phi\partial_{ext}\mathbf{d}$.

The disks that lie on the other side of Figure 29(a) match up via a parallel argument. This finishes the proof that the local contribution near d satisfies $\phi\partial_{ext}\mathbf{d} = \partial'_{ext}\phi\mathbf{d}$. The proof for d' is similar.

A similar strategy works for the case of a disk in $\partial_{ext}\mathbf{b}$. For example, suppose that c passes through the double point. Disks in the top left corner of Figure 28 contribute terms of the form $(1 + \mathbf{c})\mathbf{W}$ to $\phi\partial_{ext}\mathbf{b}$. On the other hand, since $\partial'_{ext}\mathbf{c} = 0$,

$$(50) \quad \begin{aligned} \partial'_{ext}\phi(\mathbf{b}) &= \partial'_{ext}((1 + \mathbf{c})\mathbf{b}) \\ &= (1 + \mathbf{c})\mathbf{W}. \end{aligned}$$

Note that the two \mathbf{W} terms agree because, by the arguments above, ϕ is a chain map with respect to the local contributions at negative corners. Further, if c' passes through the double point as well, then the $(1 + \mathbf{c}')$ terms in the analogue of (50) appear on the right side of \mathbf{b} . Thus, the shifts of the c and c' do not interfere with each other algebraically.

The proof for \mathbf{a} is the same. This completes the proof that $\phi\partial_{ext} = \partial'_{ext}\phi$.

$\phi\partial_{int} = \partial'_{int}\phi$: First, consider the interaction between the internal differential and ϕ on \mathbf{d} . Suppose that d passes through the double point in Figure 28. Let \tilde{d} be the d -labeled point that appears at the left of the diagram after the shift. See Figure 29. Then $\mathbf{y} = \mathbf{b}aT$ and:

$$\begin{aligned} \partial'_{int}\phi\mathbf{d} &= \partial'_{int}(\mathbf{d} + \mathbf{b}aT) \\ &= \mathbf{d}\mathbf{d} + \mathbf{d}\mathbf{b}aT + \mathbf{b}a\tilde{d}T + 2 \cdot \mathbf{b}\tilde{d}aT + \mathbf{b}a\mathbf{b}aT^2 \\ &= \phi\partial_{int}\mathbf{d}. \end{aligned}$$

The next step is to prove that $\phi\partial_{int}\mathbf{c} = \partial'_{int}\phi\mathbf{c}$. Consider the configuration in Figure 30, and, without loss of generality, suppose that c shifts to the left. Recall that \mathbf{x}_i comes from the half-flowline from c_i to the double point between c_i and d_{i-1} . The following straightforward lemma holds regardless of the labels of the points at the top and bottom of Figure 30:

Lemma 6.2.

$$\begin{aligned} \phi(\mathbf{x}_i) &= (1 + \mathbf{c}_i)^{-1}\mathbf{x}_i(1 + \mathbf{c}_i), \\ \phi(\mathbf{y}_i) &= \mathbf{y}_i. \end{aligned}$$

Now compute directly, using Lemma 6.2:

$$\begin{aligned} \phi\partial_{int}\mathbf{c}_i &= \phi((1 + \mathbf{c}_i)(\mathbf{d}_{i-1} + \mathbf{x}_i) + (\mathbf{d}_i + \mathbf{y}_i)(1 + \mathbf{c}_i)) \\ &= (1 + \mathbf{c}_i)(\mathbf{d}_{i-1} + \mathbf{y}_{i-1} + (1 + \mathbf{c}_i)^{-1}\mathbf{x}_i(1 + \mathbf{c}_i)) + \mathbf{d}_i(1 + \mathbf{c}_i) \\ &= \partial'_{int}\phi\mathbf{c}_i. \end{aligned}$$

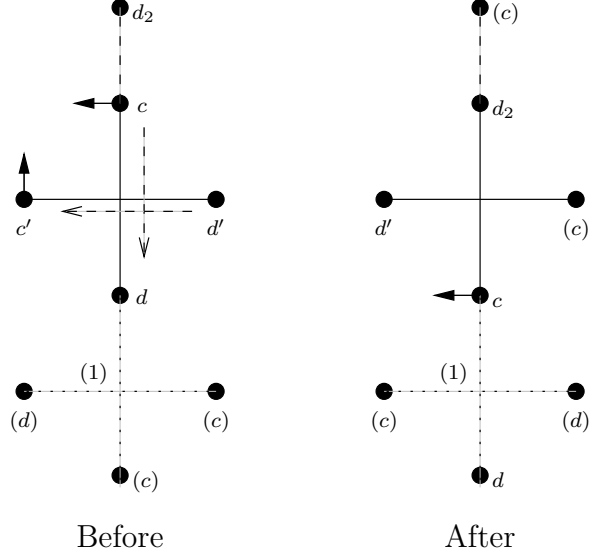


FIGURE 31. The configuration for the internal differential of \mathbf{b} when c passes through the double point. The parenthetical labels represent an arbitrary c or d label; exactly which one does not matter for this computation.

The last equality holds because after the shift, c_i is on the other side of the double point that contributes \mathbf{x}_i , but the c and d labels on the crossing strand at that double point have switched places. Thus, the double point still contributes \mathbf{x}_i . This finishes the proof for \mathbf{c} .

The internal differential on \mathbf{b} is more complicated. For simplicity, only consider the case when c and d' pass through the double point; the other cases follow from similar direct computations. Consider the configuration in Figure 31. In this case, $\mathbf{y} = \mathbf{b}_1\mathbf{a}_1T$ and $\mathbf{y}' = \mathbf{a}\mathbf{b}T$. Computing directly,

$$\begin{aligned}
 \phi\partial_{int}\mathbf{b} &= \phi(\mathbf{b}d' + \mathbf{d}\mathbf{b} + \mathbf{b}\mathbf{a}\mathbf{b}T) \\
 (51) \quad &= (1 + \mathbf{c})\mathbf{b}(d' + \mathbf{a}\mathbf{b}T) + (\mathbf{d} + \mathbf{b}_1\mathbf{a}_1T)(1 + \mathbf{c})\mathbf{b} + (1 + \mathbf{c})\mathbf{b}\mathbf{a}\mathbf{b}T \\
 &= (1 + \mathbf{c})\mathbf{b}d' + (\mathbf{d} + \mathbf{b}_1\mathbf{a}_1T)(1 + \mathbf{c})\mathbf{b}.
 \end{aligned}$$

On the other hand,

$$\begin{aligned}
 \partial'_{int}\phi(\mathbf{b}) &= \partial'_{int}((1 + \mathbf{c})\mathbf{b}) \\
 (52) \quad &= ((1 + \mathbf{c})(d_2 + \mathbf{b}\mathbf{a}T) + (\mathbf{d} + \mathbf{b}_1\mathbf{a}_1T)(1 + \mathbf{c}))\mathbf{b} \\
 &\quad + (1 + \mathbf{c})(\mathbf{b}d' + \mathbf{d}_2\mathbf{b} + \mathbf{b}\mathbf{a}\mathbf{b}T) \\
 &= (1 + \mathbf{c})\mathbf{b}d' + (\mathbf{d} + \mathbf{b}_1\mathbf{a}_1T)(1 + \mathbf{c})\mathbf{b}.
 \end{aligned}$$

If the local configuration near the double point labeled (1) changes so that the (c) is on the left before the shift, then the order of the factors in \mathbf{y} switch places and (51) and (52) still agree. Thus, $\partial'_{int}\phi(\mathbf{b}) = \phi\partial_{int}\mathbf{b}$.

The proof for \mathbf{a} is similar. This completes the proof that $\phi\partial_{int} = \partial'_{int}\phi$.

6.2. Legendrian Isotopy.

6.2.1. *Generic Isotopies.* The final part of Theorem 3.15 asserts that the stable tame isomorphism type of the DGA of a diagram of a Legendrian knot L is invariant under Legendrian isotopy.

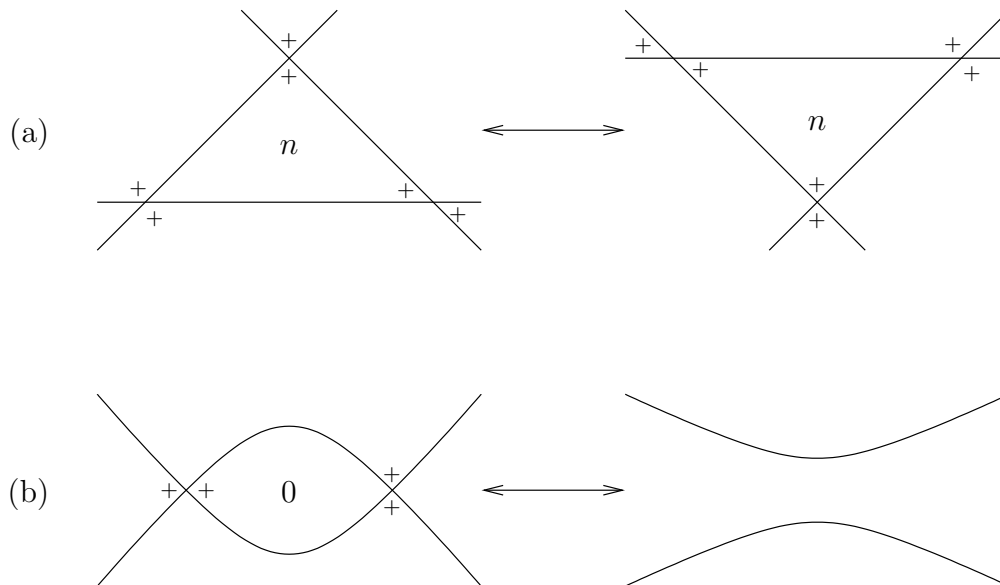


FIGURE 32. (a) The triple-point move. (b) The double-point move.

The following lemma translates Legendrian isotopy of L into combinatorial moves on the diagram (Γ_L^+, \vec{n}) :

Lemma 6.3. *If L_0 and L_1 are Legendrian isotopic Legendrian knots in E , then $(\Gamma_{L_0}^+, \vec{n}_0)$ and $(\Gamma_{L_1}^+, \vec{n}_1)$ differ by a sequence of the local moves shown in Figure 32.*

Proof. Let L_s be a Legendrian isotopy in E between L_0 and L_1 . Since the contact structure is transverse to the fibers, the isotopy projects to a homotopy of immersions $\gamma_s : S^1 \rightarrow F$, which may be assumed to be generic away from the transitions pictured in Figure 32.

The defects in Figure 32 need some justification. Since the strands of L are disjoint during both of these moves, the following inequality always holds for some fixed $\epsilon > 0$:

$$(53) \quad \epsilon < l(a_i^0) < 2\pi - \epsilon,$$

and similarly for $l(b_i^0)$.

In the case of the triple-point move, in the limit as the area of the central triangle goes to zero, the equation for the defect reads:

$$(54) \quad 2\pi n = -l(a_1^0) + l(b_2^0) + l(b_3^0).$$

Since the defect is an integer, the defect n of the central triangle in Figure 32(a) is either 0 or 1. These two cases correspond to the two types of triple point moves for Legendrian knots in \mathbb{R}^3 ; see [5, 16]. A similar argument using equation (53) shows that the defect of the central lune in Figure 32(b) must be 0. \square

The rest of this section is devoted to proving that the stable tame isomorphism type of the DGA of a knot diagram is invariant under the two moves in Figure 32.

6.2.2. Triple-Point Move. Up to choosing the position of c_1 and the transversal directions at the c points, the two possible configurations for the generators near a triple-point move are pictured in

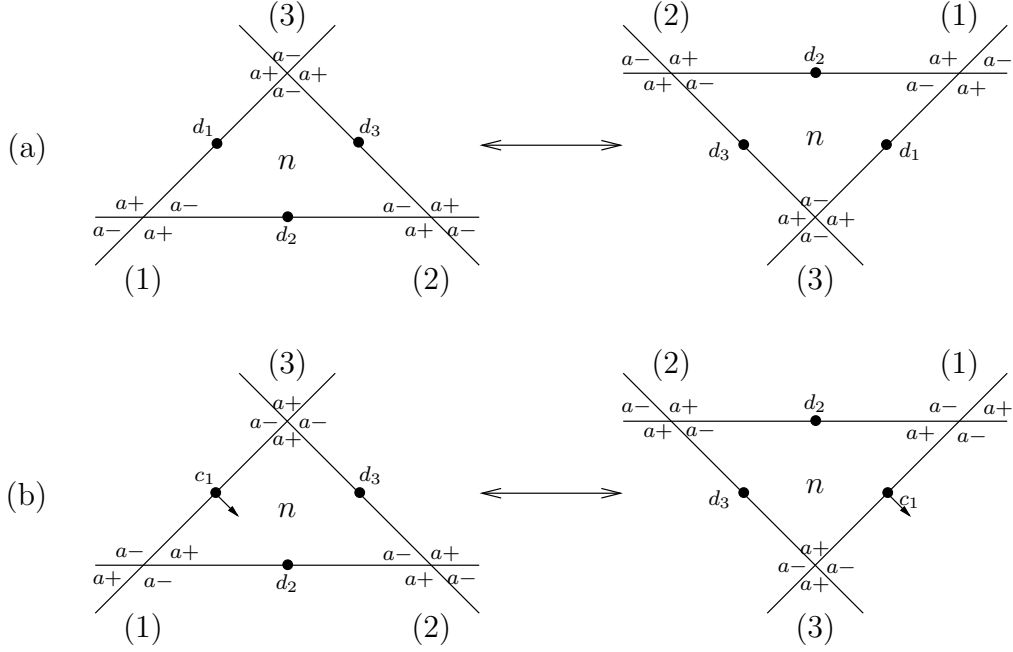


FIGURE 33. The two possible configurations of the generators near a triple point. The parenthetical numbers are labels for the double points. The DGAs for the left sides of (a) and (b) are denoted by (\mathcal{A}, ∂) , while the DGAs for the right sides are denoted by $(\mathcal{A}', \partial')$.

Figure 33. For the moment, consider only the diagrams in Figure 33(a). Define a map $\phi : \mathcal{A} \rightarrow \mathcal{A}'$ by:

$$(55) \quad \phi(\mathbf{x}) = \begin{cases} \mathbf{a}_1 + \mathbf{b}_3 \mathbf{b}_2 T^n & \mathbf{x} = \mathbf{a}_1, \\ \mathbf{a}_2 + \mathbf{b}_1 \mathbf{b}_3 T^n & \mathbf{x} = \mathbf{a}_2, \\ \mathbf{a}_3 + \mathbf{b}_2 \mathbf{b}_1 T^n & \mathbf{x} = \mathbf{a}_3, \\ \mathbf{d}_1 + \mathbf{a}_1 \mathbf{b}_1 T + \mathbf{b}_3 \mathbf{a}_3 T + \mathbf{b}_3 \mathbf{b}_2 \mathbf{b}_1 T^{n+1} & \mathbf{x} = \mathbf{d}_1, \\ \mathbf{d}_2 + \mathbf{a}_2 \mathbf{b}_2 T + \mathbf{b}_1 \mathbf{a}_1 T + \mathbf{b}_1 \mathbf{b}_3 \mathbf{b}_2 T^{n+1} & \mathbf{x} = \mathbf{d}_2, \\ \mathbf{d}_3 + \mathbf{a}_3 \mathbf{b}_3 T + \mathbf{b}_2 \mathbf{a}_2 T + \mathbf{b}_2 \mathbf{b}_1 \mathbf{b}_3 T^{n+1} & \mathbf{x} = \mathbf{d}_3, \\ \mathbf{x} & \text{otherwise.} \end{cases}$$

Lemma 6.4. *The map ϕ is a tame isomorphism of DGAs.*

Proof. The map ϕ is the composition of three tame isomorphisms of algebras:

1. $\phi_1(\mathbf{d}_i) = \mathbf{d}_i + \mathbf{a}_i \mathbf{b}_i T$ for $i = 1, 2, 3$. It is the identity on all other generators.
2. $\phi_2(\mathbf{a}_i) = \mathbf{a}_i + \mathbf{b}_{i-1} \mathbf{b}_{i-2}$, where $i - 1$ and $i - 2$ are interpreted cyclically. It is the identity elsewhere.
3. $\phi_3(\mathbf{d}_i) = \mathbf{d}_i + \mathbf{b}_{i-1} \mathbf{a}_{i-1} T$, where $i - 1$ is interpreted cyclically. It is the identity on all other generators.

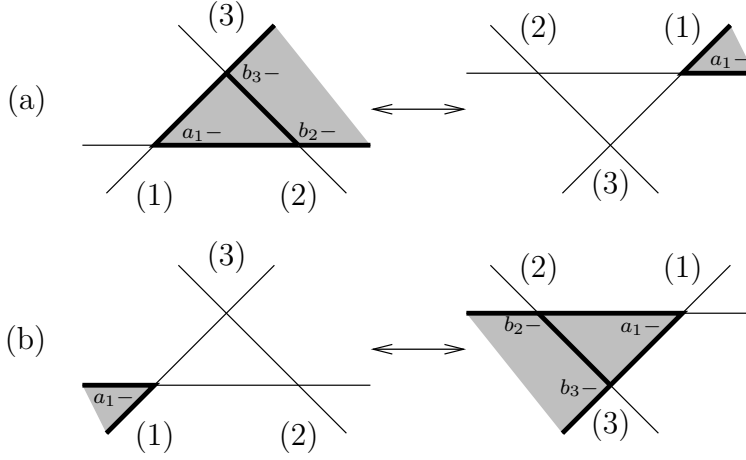


FIGURE 34. Disks for differentials of generators that lie outside the diagram.

Each of these maps preserves the filtration by Lemma 3.13. The first and last maps preserve grading since, by (14),

$$\begin{aligned} |a^k| + |b^l| &= (k + l + 1)\mu_E - 1 \\ &= |a^{k+l+1}|. \end{aligned}$$

For ϕ_2 , the fact that $\partial \mathbf{b}_1 = \mathbf{a}_2 \mathbf{a}_3 T^{1-n} + \dots$ implies

$$|b_1^{k+l+1-n}| = |a_2^k| + |a_3^l| + 1.$$

Hence, again using (14),

$$|a_1^{k+l+n}| = |b_2^k| + |b_3^l|.$$

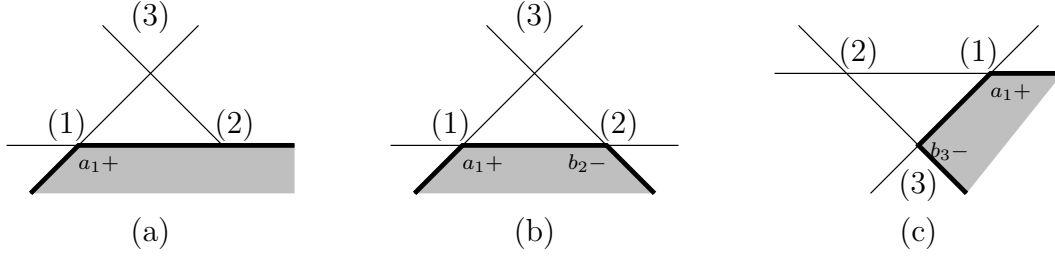
It follows that ϕ itself is a tame isomorphism of filtered graded algebras.

Let \mathbf{x} be a generating power series for a special point that lies outside of Figure 33. To show that ϕ is a chain map on \mathbf{x} with respect to ∂_{ext} , consider the disks in Figure 34. The disks in $\partial_{ext} \mathbf{x}$ shown in Figure 34(a) give rise to terms containing $\mathbf{a}_1 + \mathbf{b}_3 \mathbf{b}_2 T^n$. The $\mathbf{b}_3 \mathbf{b}_2 T^n$ term in $\phi(\mathbf{a}_1)$ cancels the one in $\partial_{ext} \mathbf{x}$, so the image under ϕ of the terms coming from the left side of Figure 34(a) correspond precisely to the terms in $\partial'_{ext} \mathbf{x}$ coming from the right side. For the disks pictured in Figure 34(b), $\partial_{ext} \mathbf{x}$ has terms with \mathbf{a}_1 in them, while $\partial'_{ext} \mathbf{x}$ has terms with $\mathbf{a}_1 + \mathbf{b}_3 \mathbf{b}_2 T^n$. This time, ϕ inserts $\mathbf{b}_3 \mathbf{b}_2 T^n$ into $\partial_{ext} \mathbf{x}$ to give $\partial'_{ext} \mathbf{x}$. Symmetric arguments apply to disks in $\partial_{ext} \mathbf{x}$ that differ by a rotation from those in Figure 34.

The map ϕ only affects $\partial_{int} \mathbf{x}$ if x is a c generator situated immediately outside the diagram. Suppose that c lies on the upper right strand of Figure 33. Calculate directly with the flowlines that appear in the figure:

$$\begin{aligned} \phi \partial_{int} \mathbf{c} &= \phi((1 + \mathbf{c})(\mathbf{d}_1 + \mathbf{b}_3 \mathbf{a}_3 T)) \\ &= (1 + \mathbf{c})((\mathbf{d}_1 + \mathbf{a}_1 \mathbf{b}_1 T + \mathbf{b}_3 \mathbf{a}_3 T + \mathbf{b}_3 \mathbf{b}_2 \mathbf{b}_1 T^{n+1}) \\ &\quad + (\mathbf{b}_3 \mathbf{a}_3 T + \mathbf{b}_3 \mathbf{b}_2 \mathbf{b}_1 T^{n+1})) \\ &= (1 + \mathbf{c})(\mathbf{d}_1 + \mathbf{a}_1 \mathbf{b}_1 T) \\ &= \partial'_{int} \phi \mathbf{c}. \end{aligned}$$

The other cases are symmetric, so ϕ is a chain map on \mathbf{x} .

FIGURE 35. (a and b) \mathbf{U}_{ext} ; (c) \mathbf{V}_{ext} .

Next, consider the generating power series \mathbf{a}_1 ; as usual, the proofs for the other \mathbf{a}_i are symmetric. The left- and right-hand sides of the equation $\phi\partial\mathbf{a}_1 = \partial'\phi\mathbf{a}_1$ may be broken up as follows:

$$(56) \quad \begin{aligned} \phi\partial\mathbf{a}_1 &= \mathbf{U}_{int} + \mathbf{U}_{ext}, \\ \partial'\phi\mathbf{a}_1 &= \mathbf{V}_{int} + \mathbf{V}_{ext} + \mathbf{W}_{int} + \mathbf{W}_{ext} + \mathbf{W}_\Delta. \end{aligned}$$

The terms are:

$\mathbf{U}_{int}, \mathbf{U}_{ext}$: the terms that make up $\phi\partial_{int}\mathbf{a}_1$ and $\phi\partial_{ext}\mathbf{a}_1$, respectively.

$\mathbf{V}_{int}, \mathbf{V}_{ext}$: the terms that make up $\partial'_{int}\mathbf{a}_1$ and $\partial'_{ext}\mathbf{a}_1$, respectively.

\mathbf{W}_{int} : the terms that make up $\partial'_{int}(\mathbf{b}_3\mathbf{b}_2T^n)$.

\mathbf{W}_{ext} : the terms that make up $\partial'_{ext}(\mathbf{b}_3\mathbf{b}_2T^n)$ except those that come from the central triangle in Figure 33.

\mathbf{W}_Δ : the remaining terms in $\partial'_{ext}(\mathbf{b}_3\mathbf{b}_2T^n)$ that come from the central triangle.

Claim 6.5. *The terms in \mathbf{U}_{ext} correspond to those in $\mathbf{V}_{ext} + \mathbf{W}_{ext}$.*

Half of the disks in $\partial_{ext}\mathbf{a}_1$ are pictured in Figure 35(a,b); the other half are reflections of those in the figure across the line through a_1 and d_2 . The terms represented by the disks in Figure 35(a) are unchanged both by the triple-point move and by ϕ , and hence appear in both \mathbf{U}_{ext} and \mathbf{V}_{ext} .¹⁴ The disks that appear in Figure 35(b) give rise to terms of the form $\mathbf{U}\mathbf{b}_2$. On the other hand, the disks in \mathbf{V}_{ext} are of the form $\mathbf{b}_3\mathbf{V}$, as shown in Figure 35(c). By the Leibniz rule for ∂'_{ext} , \mathbf{W}_{ext} consists of terms of the form $\mathbf{U}\mathbf{b}_2 + \mathbf{b}_3\mathbf{V}$. The defect for the \mathbf{U} term in \mathbf{W}_{ext} differs from that of the $\mathbf{U}\mathbf{b}_2$ term in \mathbf{U}_{ext} by T^{-n} , so the exponents of T agree. This finishes the proof of the claim.

Claim 6.6. *The terms in \mathbf{U}_{int} correspond with those in $\mathbf{V}_{int} + \mathbf{W}_{int} + \mathbf{W}_\Delta$.*

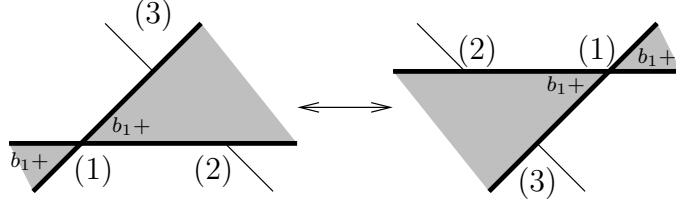
The claim follows from direct computation:

$$\begin{aligned} \mathbf{U}_{int} &= \phi(\mathbf{d}_1\mathbf{a}_1 + \mathbf{a}_1\mathbf{d}_2) \\ &= (\mathbf{d}_1\mathbf{a}_1 + \mathbf{a}_1\mathbf{d}_2) + (\mathbf{b}_3\mathbf{a}_3\mathbf{a}_1T + \mathbf{a}_1\mathbf{a}_2\mathbf{b}_2T) \\ &\quad + (\mathbf{d}_1\mathbf{b}_3\mathbf{b}_2 + \mathbf{b}_3\mathbf{b}_2\mathbf{d}_2 + \mathbf{b}_3\mathbf{a}_3\mathbf{b}_3\mathbf{b}_2T + \mathbf{b}_3\mathbf{b}_2\mathbf{a}_2\mathbf{b}_2T)T^n \\ &= \mathbf{V}_{int} + \mathbf{W}_\Delta + \mathbf{W}_{int}. \end{aligned}$$

This finishes the proof that ϕ is a chain map on \mathbf{a}_1 .

Next, consider the generating power series \mathbf{b}_1 . Aside from the terms that do not come from the inner triangle, the external differentials before and after the triple-point move come from the disks pictured in Figure 36. These disks are unchanged by the triple-point move and by ϕ .

¹⁴For disks in $\partial_{ext}\mathbf{a}_1$ that come back to the triple point, use the arguments for \mathbf{x} above.


 FIGURE 36. The disks involved in $\partial_{ext}\mathbf{b}_1$.

For the internal differentials and the terms of the external differential that come from the inner triangle, compute:

$$\begin{aligned}\phi\partial\mathbf{b}_1 &= \phi(\mathbf{b}_1\mathbf{d}_1 + \mathbf{d}_2\mathbf{b}_1 + \mathbf{b}_1\mathbf{a}_1\mathbf{b}_1T + \mathbf{a}_2\mathbf{a}_3) \\ &= \mathbf{b}_1\mathbf{d}_1 + \mathbf{d}_2\mathbf{b}_1 + \mathbf{b}_1\mathbf{a}_1\mathbf{b}_1T + \mathbf{a}_2\mathbf{a}_3 \\ &= \partial'\phi\mathbf{b}_1.\end{aligned}$$

Despite appearances, the equality between the first and second lines involves some cancellations. This completes the proof that ϕ is a chain map on \mathbf{b}_1 .

The calculation for the generating power series \mathbf{d}_i is similar to that for the \mathbf{a}_i and \mathbf{b}_i generating power series. Lemma 6.4 follows. \square

For the second case in Figure 33, the tame isomorphism is given by:

$$(57) \quad \phi(\mathbf{x}) = \begin{cases} \mathbf{a}_1(1 + \mathbf{c}_1) & \mathbf{x} = \mathbf{a}_1 \\ \mathbf{a}_2 + \mathbf{a}_1(1 + \mathbf{c}_1)\mathbf{a}_3 & \mathbf{x} = \mathbf{a}_2 \\ (1 + \mathbf{c}_1)\mathbf{a}_3 & \mathbf{x} = \mathbf{a}_3 \\ (1 + \mathbf{c}_1)^{-1}(\mathbf{b}_1 + (1 + \mathbf{c}_1)\mathbf{a}_3\mathbf{b}_2) & \mathbf{x} = \mathbf{b}_1 \\ \mathbf{b}_3(1 + \mathbf{c}_1)^{-1} + \mathbf{b}_2\mathbf{a}_1 & \mathbf{x} = \mathbf{b}_3 \\ \mathbf{d}_2 + \mathbf{a}_1\mathbf{b}_1 + (\mathbf{a}_2 + \mathbf{a}_1(1 + \mathbf{c}_1)\mathbf{a}_3)\mathbf{b}_2 & \mathbf{x} = \mathbf{d}_2 \\ \mathbf{d}_3 + \mathbf{b}_2\mathbf{a}_2 + (\mathbf{b}_3(1 + \mathbf{c})^{-1} + \mathbf{b}_2\mathbf{a}_1)(1 + \mathbf{c})\mathbf{a}_3 & \mathbf{x} = \mathbf{d}_2 \\ \mathbf{x} & \text{otherwise.} \end{cases}$$

The proof that this is a tame isomorphism of DGAs is similar to the proof of Lemma 6.4.

6.2.3. Double-Point Move. The last step in proving Theorem 3.15 is to show that the double point move does not change the stable tame isomorphism type of a knot diagram's DGA. Up to a choice of transverse directions at the c points and an overall shift in the c and d labels, there are two possibilities for the labeling of the diagram; see Figure 37. Only the first possibility is considered in this section; the proof for the second is almost identical.

Let (\mathcal{A}, ∂) be the DGA for the diagram on the left of Figure 37(a), and let $(\mathcal{A}', \partial')$ be the DGA for the diagram on the right. Define the following four stabilizations:

1. $\mathcal{E}_1 = \mathcal{E}(\boldsymbol{\alpha}_2, \boldsymbol{\beta}_1)$, with grading given by $|\beta_1^k| = |b_1^k|$.
2. $\mathcal{E}_2 = \mathcal{E}(\boldsymbol{\alpha}_1, \boldsymbol{\beta}_2)$, with grading given by $|\beta_2^k| = |b_2^k|$.
3. $\mathcal{E}_3 = \mathcal{E}(\boldsymbol{\delta}_1, \boldsymbol{\gamma}_1)$, with grading given by $|\gamma_1^k| = |c_1^k|$.
4. $\mathcal{E}_4 = \mathcal{E}(\boldsymbol{\delta}_2, \boldsymbol{\gamma}_2)$, with grading given by $|\gamma_2^k| = |c_2^k|$.

Let $(S(\mathcal{A}'), \partial')$ be the result of stabilizing \mathcal{A}' with $\mathcal{E}_1, \dots, \mathcal{E}_4$. The rest of this section will carry out a five-step program to show that (\mathcal{A}, ∂) is tame isomorphic to $(S(\mathcal{A}'), \partial')$. The first steps construct four intermediate DGAs $(\mathcal{A}_i, \partial_i)$, $i = 1, \dots, 4$, that are stable tame isomorphic to (\mathcal{A}, ∂) ; the last step shows that $(\mathcal{A}_4, \partial_4) \simeq (S(\mathcal{A}'), \partial')$.

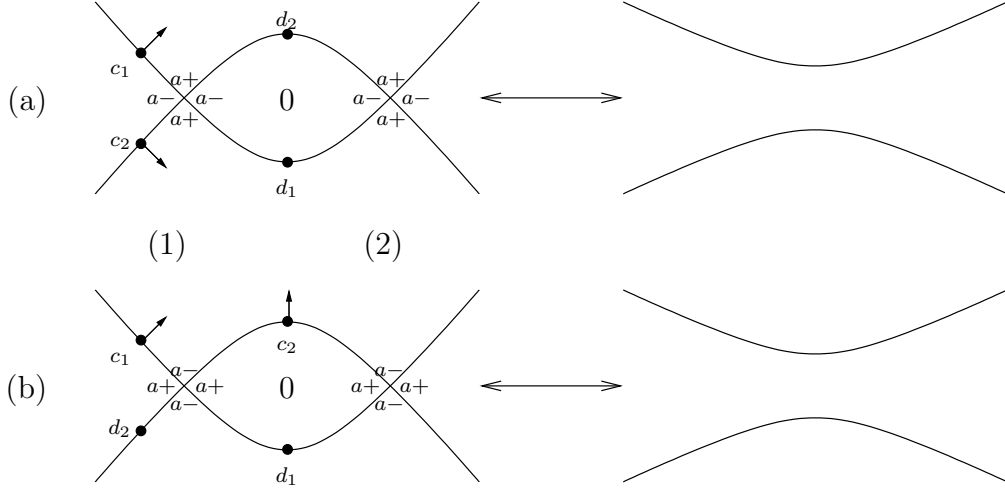


FIGURE 37. Two types of possible diagrams for the double-point move.

Step 1

Let $\hat{\mathcal{A}}$ be an algebra generated by the same power series (except for \mathbf{a}_2 and \mathbf{b}_1) as \mathcal{A} .

Definition 6.7. As an algebra, $\mathcal{A}_1 = S_{\mathcal{E}_1}(\hat{\mathcal{A}})$.

To define a differential on \mathcal{A}_1 , let $W^k \in \mathcal{A}$ be given by:

$$(58) \quad \partial b_1^k = a_2^k + W^k$$

Define $W_R^k \in \mathcal{A}_1$ by the following inductive procedure: first, let $W_R^0 = W^0$. Since the curvature over the lune in Figure 37 is arbitrarily small, $l(a_2^k)$ is arbitrarily close to $l(b_1^k)$. Thus, any generator w that appears in W^k must satisfy $l(w) < l(a_2^k)$. In particular, any generator a_2^j appearing in W^k must have $j < k$. To define W_R^k , replace any a_2^j that appears in W^k by W_R^j and any b_1^j by 0.

Definition 6.8. The differential ∂_1 on \mathcal{A}_1 is

$$(59) \quad \partial_1 \mathbf{x} = \partial \mathbf{x} \Big|_{\substack{a_2^k = W_R^k \\ b_1^k = 0}} \quad \text{for all } k \geq 0.$$

That $\partial_1 \circ \partial_1 = 0$ will be proven by showing that there is a tame isomorphism Φ_1 of algebras between \mathcal{A} and \mathcal{A}_1 that intertwines ∂ and ∂_1 . In order to define Φ_1 , construct a sequence of algebras \mathcal{A}^k , $k = 0, 1, \dots$, where:

$$(60) \quad F^j \mathcal{A}^k = \begin{cases} F^j \mathcal{A}_1 & 0 \leq j < k, \\ F^j \mathcal{A} & j \geq k. \end{cases}$$

In other words, the generators a_2^0, \dots, a_2^{k-1} in \mathcal{A} are replaced by $\alpha_2^0, \dots, \alpha_2^{k-1}$ and the generators b_1^0, \dots, b_1^{k-1} are replaced by $\beta_1^0, \dots, \beta_1^{k-1}$. Furthermore, $\mathcal{A}^0 = \mathcal{A}$ and \mathcal{A}_1 is the direct limit of the \mathcal{A}^k . Each algebra in the sequence has a differential defined by:

$$(61) \quad \partial^k \mathbf{x} = \partial \mathbf{x} \Big|_{\substack{a_2^j = W_R^j \\ b_1^j = 0}}$$

for $j = 0, 1, \dots, k-1$. Note that the projection operator $\tau : \mathcal{A}_1 \rightarrow \hat{\mathcal{A}}$ and the homotopy operator $H : \mathcal{A}_1 \rightarrow \mathcal{A}_1$ defined in Section 3.4 descend to the algebras \mathcal{A}^k . They still satisfy:

$$(62) \quad \tau \circ i + Id_{\hat{\mathcal{A}}} = H \circ \partial^k + \partial^k \circ H.$$

The next step in defining Φ_1 is to construct tame isomorphisms $\phi^k : \mathcal{A}^k \rightarrow \mathcal{A}^{k+1}$. First, define an order \prec on the generators of \mathcal{A}^k by length, with $d^j \prec c^j$ and with α_2^j and β_1^j replacing a_2^j and b_1^j , respectively, in the ordering. Make the curvature of the lune small enough so that there are no generators that lie between a_2^k and b_1^k . Lemma 3.9 and the definition of ∂_{int} then imply that every generator that appears in $\partial^k x$ precedes x in the ordering.

Define $\phi_0^k : \mathcal{A}_1^k \rightarrow \mathcal{A}_1^{k+1}$ by:

$$(63) \quad \phi_0^k(x^j) = \begin{cases} \beta_1^k & x^j = b_1^k, \\ \alpha_2^k + W_R^k & x^j = a_2^k, \\ x^j & \text{otherwise.} \end{cases}$$

This is an elementary isomorphism. Next, use this map to define $\phi^k : \mathcal{A}^k \rightarrow \mathcal{A}^{k+1}$ by:

$$(64) \quad \phi^k(x^j) = \begin{cases} \phi_0^k(x^j) & x^j = a_2^k, b_1^k, \\ x^j & x^j = \alpha_2^j, \beta_1^j, \\ x^j + H\phi_0^k\partial^k x^j & \text{otherwise.} \end{cases}$$

Lemma 6.9. *The map ϕ^k is a tame isomorphism of algebras that satisfies*

$$(65) \quad \partial^{k+1}\phi^k = \phi^k\partial^k.$$

In particular, ∂^k is a differential on \mathcal{A}^k .

Proof. The map ϕ^k is a tame isomorphism of algebras by the remark after Lemma 3.13.

To prove (65), there are four types of generators x^j to consider: $x^j \prec a_2^k$, $x^j = a_2^k$, $x^j = b_1^k$, and $x^j \succ b_1^k$. The case when $x^j \prec a_2^k$ follows from two facts. First, a_2^k does not appear in $\partial^k x^j$ for all $l \leq j$. Thus, $H\phi_0^k\partial^k x^j = 0$, and hence $\phi^k(x^j) = x^j$. Second, $\partial^{k+1}x^j = \partial^k x^j$ for $j \leq k$. Putting these together yields:

$$\begin{aligned} \partial^{k+1}\phi^k x^j &= \partial^{k+1}x^j && \text{by the first fact} \\ &= \partial^k x^j && \text{by the second fact} \\ &= \phi^k\partial^k x^j && \text{by the first fact.} \end{aligned}$$

This proves the first case.

For the second case, the following lemma is required:

Lemma 6.10. $\partial_1 a_2^k = \partial_1 W_R^k$.

Proof. Since $\partial \circ \partial = 0$, (58) implies, for all k , that:

$$(66) \quad \partial a_2^k = \partial W^k.$$

The remainder of the proof is an induction on k . For $k = 0$, $W^0 = W_R^0$ by definition. Thus, $\partial_1 W^0 = \partial_1 W_R^0$. In general, a typical term in W^k has the form $x_1 a_2^{j_1} x_2 \cdots x_n a_2^{j_n} x_{n+1}$ with $j_i < k$.

In W_R^k , this term becomes $x_1 W_R^{j_1} x_2 \cdots x_n W_R^{j_n} x_{n+1}$. The Leibniz rule and the inductive hypothesis imply:

$$\begin{aligned} \partial_1(x_1 a_2^{j_1} x_2 \cdots x_n a_2^{j_n} x_{n+1}) &= (\partial(x_1) a_2^{j_1} \cdots + x_1 \partial(a_2^{j_1}) \cdots + \cdots) \Big|_{\substack{a_2^j = W_R^j \\ b_1^j = 0}} \\ &= \partial(x_1) W_R^{j_1} \cdots + x_1 \partial(W_R^{j_1}) \cdots + \cdots \\ &= \partial_1(x_1 W_R^{j_1} x_2 \cdots x_n W_R^{j_n} x_{n+1}). \end{aligned}$$

□

To complete the second case, compute directly:

$$\begin{aligned} \partial^{k+1} \phi^k a_2^k &= \partial^{k+1} (\alpha_2^k + W_R^k) \\ &= \partial^{k+1} W_R^k && \text{since } \partial^{k+1} \alpha_2^k = 0; \\ &= \phi^k \partial^k W_R^k && \text{by the proof of the first case;} \\ &= \phi^k \partial^k a_2^k && \text{by Lemma 6.10.} \end{aligned}$$

The third case also follows from a straightforward computation.

For the final case, proceed by induction on the order \prec . To begin, use (62) to get:

$$\phi^k \partial^k x^j = \tau \phi^k \partial^k x^j + \partial^{k+1} H \phi^k \partial^k x^j + H \partial^{k+1} \phi^k \partial^k x^j.$$

Lemma 3.9, the definition of ∂_{int} and the inductive hypothesis give:

$$= \tau \phi^k \partial^k x^j + \partial^{k+1} H \phi^k \partial^k x^j + H \phi^k \partial^k \partial^k x^j.$$

For every a_2^k appearing in the image of ∂^k , $\tau \phi^k$ substitutes in W_R^k . This is the same as $\tau \partial^{k+1}$. Thus:

$$= \tau \partial^{k+1} x^j + \partial^{k+1} H \phi^k \partial^k x^j.$$

Another application of (62) gives:

$$= \partial^{k+1} (x^j + H(\partial^{k+1} x^j + \phi^k \partial^k x^j)) + H \partial^{k+1} \partial^{k+1} x^j.$$

The second and last terms disappear, leaving:

$$= \partial^{k+1} \phi^k x^j.$$

This completes the final case, and hence the proof of the lemma. □

With this machinery in hand, define $\Phi_1 : \mathcal{A} \rightarrow \mathcal{A}_1$ by:

$$(67) \quad \Phi_1 = \cdots \circ \phi^2 \circ \phi^1 \circ \phi^0.$$

The map Φ_1 satisfies the finiteness requirement for a tame isomorphism of algebras since ϕ^k is the identity on $F^{k-1} \mathcal{A}$. That Φ_1 is a tame isomorphism of DGAs follows from Lemma 6.9.

Steps 2, 3, and 4

Let $\hat{\mathcal{A}}_1$ be generated by the same power series (except for \mathbf{a}_1 and \mathbf{b}_2) as \mathcal{A}_1 . Suppose that:

$$(68) \quad \partial_1 b_2^k = a_1^k + V^k.$$

Define V_R^k from V^k by the same inductive procedure that produced W_R^k .

Definition 6.11. As an algebra, $\mathcal{A}_2 = \mathcal{S}_{\mathcal{E}_2}(\hat{\mathcal{A}}_1)$. The differential ∂_2 on \mathcal{A}_2 is defined by:

$$(69) \quad \partial_2 \mathbf{x} = \partial_1 \mathbf{x} \Big|_{\substack{a_1^k = V_R^k \\ b_2^k = 0}}$$

for all $k \geq 0$.

The same procedure as in Step 1 provides a tame isomorphism Φ_2 between $(\mathcal{A}_1, \partial_1)$ and $(\mathcal{A}_2, \partial_2)$.

Build $(\mathcal{A}_3, \partial_3)$ and $(\mathcal{A}_4, \partial_4)$ in much the same way: first repeat the construction on \mathcal{A}_2 with c_1 in the place of b_1 , d_1 in the place of a_2 , and X_R^k in the place of V_R^k to obtain $(\mathcal{A}_3, \partial_3)$. Note that X_R^k comes from flowlines that start at c_1 and leave Figure 37 along the upper left strand. Again, there exists a tame isomorphism $\Phi_3 : (\mathcal{A}_2, \partial_2) \rightarrow (\mathcal{A}_3, \partial_3)$.

Next, repeat the construction on \mathcal{A}_3 with c_2 in the place of c_1 , d_2 in the place of d_1 , and Y_R^k in the place of X_R^k to obtain $(\mathcal{A}_4, \partial_4)$. As before, there exists a tame isomorphism $\Phi_4 : (\mathcal{A}_3, \partial_3) \rightarrow (\mathcal{A}_4, \partial_4)$.

Step 5

The final step is to show that $\mathcal{A}_4 \simeq S(\mathcal{A}')$ as DGAs. They have the same generators by construction, so they are isomorphic as algebras; it remains to show that $\partial_4 = \partial'$.

Let x^k be a generator of \mathcal{A} that does not appear in Figure 37. Write the differential of x^k in \mathcal{A} as:

$$(70) \quad \partial x^k = W_0 + W_1 + W_{int} + W_{ext}.$$

The terms on the right hand side are as follows:

- W_0 consists of words that do not contain any of the generators that appear in the left hand side of Figure 37(a).
- W_1 consists of words that contain either b_i^j or c_i^j , $i = 1, 2$.
- W_{int} consists of words in $\partial_{int}(x^k)$ that contain d_i^j , $i = 1, 2$.
- W_{ext} consists of words in $\partial_{ext}(x^k)$ that contain a_i^j but not b_i^j or c_i^j , $i = 1, 2$.

Similarly, the differential of x^k in \mathcal{A}' may be written as:

$$(71) \quad \partial' x^k = W_0 + W'_{int} + W'_{ext}.$$

The two new terms on the right hand side are:

- W'_{int} , consisting of words coming from flowlines that pass through the right hand side of Figure 37(a); and
- W'_{ext} , consisting of words coming from disks that pass “through the neck” of the right hand side of Figure 37.

The task is to prove that, under the substitutions in Steps 1 through 4 that transform ∂ into ∂_4 , $W_1 + W_{int} + W_{ext}$ becomes $W'_{int} + W'_{ext}$.

First of all, all words in W_1 contain generators that get mapped to 0 by one of $\partial_1, \dots, \partial_4$. Hence, W_1 does not appear in $\partial_4 x^k$ in any form.

Secondly, W_{int} transforms into W'_{int} . To see this, consider the case of a generator that lies just off of the top right corner of Figure 37(a).¹⁵ The terms with d_1^k in W_{int} are untouched until Step 3, when d_1^k is replaced by X_R^k . As noted above, X_R^k comes from flowlines that leave Figure 37(a) via the top left strand. The result of the substitution of X_R^k for d_1^k , then, is that the flowlines coming into d_1 from the right are glued to flowlines leaving c_1 to the left. As shown in Figure 38, these form flowlines that pass through the diagram in Figure 37(a). These are precisely the flowlines that give W'_{int} .

¹⁵The case of a generator that lies off of the bottom right corner is symmetric. The interior differentials of generators off of the left side do not involve any of the generators in Figure 37(a).

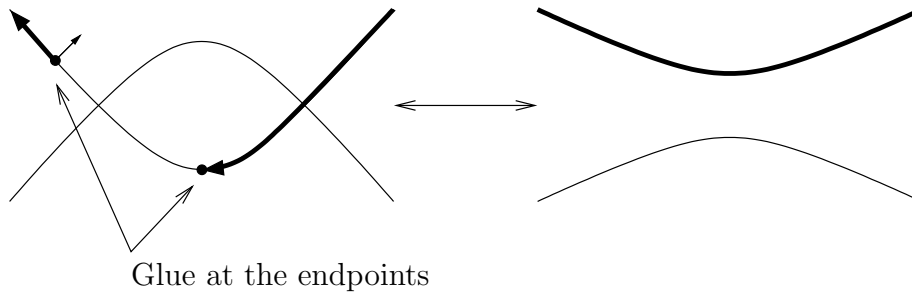


FIGURE 38. Gluing two flowlines together to form a flowline that passes through the diagram.

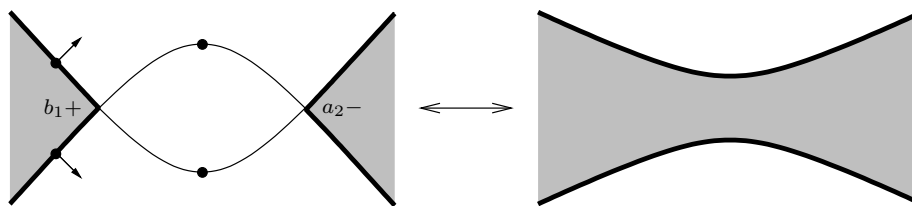


FIGURE 39. Gluing two disks together to get a disk that passes through the neck.

Thirdly, W_{ext} transforms into W'_{ext} . For conceptual clarity, assume that W_{ext} and W_R^k are both monomials, i.e. each comes from a single disk. The general case is a sum over all the disks involved in the constructions described below. The first step is to describe W_R^k geometrically. Recall that in the inductive definition of W_R^k , every occurrence of a_2^j in W is replaced by W_R^j . The substitution of W_R^j can be represented geometrically by the gluing pictured in Figure 39. Thus, W_R^k should be thought of as a disk that passes through the neck on the right side of Figure 39 (possibly multiple times) that has a “phantom” positive corner at b_1^j that can be glued to a negative corner at a_2^j . The construction of V_R^j is similar.

With the geometric description of W_R^k in hand, suppose that W_{ext} has a negative corner at a_2^j . In the definition of ∂_1 , a_2^j is replaced by W_R^j . As before, this is the algebraic realization of gluing W_R^j to W_{ext} as in Figure 39. After replacing all generators a_2^j with W_R^j and a_1^j with V_R^j , the result is a disk that passes through the neck (possibly multiple times). In other words, the result is a summand of W'_{ext} . Conversely, any disk in W_{ext} may be constructed in this manner by squeezing off the neck of a disk in W'_{ext} . Thus, $\partial_4 x^k = \partial' x^k$.

Finally, since $\partial_4 = \partial'$ on the α , β , γ , and δ generators, the arguments above show that $\partial_4 = \partial'$ on all of $S(\mathcal{A}')$. This finishes the proof that \mathcal{A}_4 is tame isomorphic to $S(\mathcal{A}')$ as DGAs, and hence the proof of Theorem 3.15.

ACKNOWLEDGMENTS

This paper stems from my thesis research, and I would like to thank Yasha Eliashberg for his insight and expert guidance. Additionally, I have benefited greatly from discussions and correspondence with Lenny Ng, John Etnyre, and Frederic Bourgeois.

REFERENCES

- [1] B. Aebischer et al., *Symplectic geometry*, Prog. Math., vol. 124, Birkhäuser, 1994.

- [2] D. M. Austin and P. J. Braam, *Morse-Bott theory and equivariant cohomology*, The Floer Memorial Volume, Birkhäuser, Basel, 1995, pp. 123–183.
- [3] D. Bennequin, *Entrelacements et equations de Pfaff*, Asterisque **107–108** (1983), 87–161.
- [4] F. Bourgeois, *A Morse-Bott approach to contact homology*, Preprint, 2002.
- [5] Yu. Chekanov, *Differential algebras of Legendrian links*, Invent. Math. (2002), To Appear.
- [6] Y. Eliashberg, *Classification of overtwisted contact structures on 3-manifolds*, Invent. Math. **98** (1989), no. 3, 623–637.
- [7] ———, *Filling by holomorphic discs and its applications*, Geometry of low-dimensional manifolds, 2 (Durham, 1989), Cambridge Univ. Press, Cambridge, 1990, pp. 45–67.
- [8] ———, *Contact 3-manifolds twenty years since J. Martinet's work*, Ann. Inst. Fourier (Grenoble) **42** (1992), no. 1-2, 165–192.
- [9] ———, *Legendrian and transversal knots in tight contact 3-manifolds*, Topological methods in modern mathematics (Stony Brook, NY, 1991), Publish or Perish, Houston, TX, 1993, pp. 171–193.
- [10] Y. Eliashberg and M. Fraser, *Classification of topologically trivial Legendrian knots*, Geometry, topology, and dynamics (Montreal, PQ, 1995), Amer. Math. Soc., Providence, RI, 1998, pp. 17–51.
- [11] Y. Eliashberg, A. Givental, and H. Hofer, *Introduction to symplectic field theory*, Geom. Funct. Anal. (2000), no. Special Volume, Part II, 560–673, GAFA 2000 (Tel Aviv, 1999).
- [12] Y. Eliashberg and W. Thurston, *Confoliations*, American Mathematical Society, Providence, RI, 1998.
- [13] Judith Epstein, Dmitry Fuchs, and Maike Meyer, *Chekanov-Eliashberg invariants and transverse approximations of Legendrian knots*, Pacific J. Math. **201** (2001), no. 1, 89–106.
- [14] J. Etnyre and K. Honda, *On the non-existence of tight contact structures*, Ann. Math. (2) **153** (2001), 749–766.
- [15] ———, *Knots and contact geometry*, J. Symplectic Geom. **1** (2002), X–Y.
- [16] J. Etnyre, L. Ng, and J. Sabloff, *Invariants of Legendrian knots and coherent orientations*, J. Symplectic Geom. **1** (2002), no. 2, 321–368.
- [17] J. Etnyre, *Introductory lectures on contact geometry*, Preprint, 2001.
- [18] D. Fuchs, *Chekanov-Eliashberg invariants of Legendrian knots: Existence of augmentations*, Preprint, 2000.
- [19] E. Giroux, *Structures de contact sur les variétés fibrées en cercles au-dessus d'une surface*, Comment. Math. Helv. **76** (2001), no. 2, 218–262.
- [20] K. Honda, *On the classification of tight contact structures. II*, J. Differential Geom. **55** (2000), no. 1, 83–143.
- [21] R. Lutz, *Structures de contact sur les fibres principales en cercles de dimension trois*, Ann. Inst. Fourier, Grenoble **27** (1977), no. 3, 1–15.
- [22] L. Ng, *Computable Legendrian invariants*, Topology (2002), To Appear.
- [23] A. Sato and T. Tsuboi, *Contact structures of closed manifolds fibered by the circles*, Mem. Inst. Sci. Tech. Meiji Univ. **33** (1994), 41–46.
- [24] Matthias Schwarz, *Morse homology*, Birkhäuser Verlag, Basel, 1993.
- [25] V. Turaev, *Shadow links and face models of statistical mechanics*, J. Differential Geom. **36** (1992), no. 1, 35–74.

UNIVERSITY OF PENNSYLVANIA, PHILADELPHIA, PA 19104

E-mail address: sabloff@math.upenn.edu

URL: <http://math.upenn.edu/~sabloff>